Nano Research

Open Access

Review Article

Programming ionic covalent organic framework solid-state electrolytes for rechargeable batteries: From 2D to 3D

Qingyu Dai[1], Yan Wang[1], Zhangyu Zheng[1], Yongjie Cao[2], Changding Wang[3], Dongli Xin[3] ✉, Qi Kang[3] ✉, Lianbo Ma[1] ✉, and Jie Xu[1] ✉

[1] *School of Materials Science and Engineering, Anhui University of Technology, Ma'anshan 243002, China*
[2] *Shanghai Key Laboratory of Molecular Catalysis and Innovative Materials, Institute of New Energy, Collaborative Innovation Center of Chemistry for Energy Materials (iChEM), Department of Chemistry, Fudan University, Shanghai 200433, China*
[3] *Institute of Future Technology, Southwest Jiaotong University, Chengdu 611756, China*

Cite this article: *Nano Research*, **2026**, *19*, 94908567. https://doi.org/10.26599/NR.2026.94908567

ABSTRACT: Covalent organic frameworks (COFs) are revolutionizing the solid-state ionics by programming backbone, incorporating functional groups, and chelating with specific ions in structural units to facilitate rapid ion transport. More encouragingly, topology diagrams enable COFs with tremendous possibilities in structural design from two-dimensional (2D) to three-dimensional (3D) polygonal network, thus positioning themselves as promising ionic solid-state electrolytes for energy storage and conversion. This review summarizes recent advances in COF electrolytes from 2D to 3D, focusing on how pore topology, framework functionality, and composite designs regulate Li^+ conduction. Mechanistic insights including anion immobilization, backbone–ion interactions, and solvent- or polymer-assisted transport are discussed to elucidate the structure–transport correlations that govern ionic conductivity and interfacial behavior. Key limitations, such as modest intrinsic conductivity, electrode interfacial resistance, and mechanical fragility, are critically examined. Beyond lithium systems, the broader potential of COFs as versatile solid-state ionic conductors for emerging metal-ion batteries is highlighted. Finally, future opportunities are outlined, including ionic-backbone engineering, nanochannel ordering, quasi-solid architectures, dendrite-regulating interfaces, and scalable membrane processing. We earnestly expect that this review will further elucidate pathways for the advancement of COF-based electrolytes toward practical and high-performance solid-state rechargeable batteries.

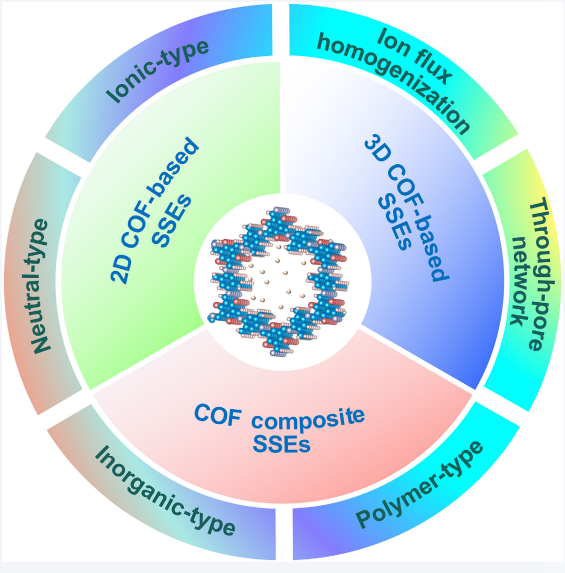

KEYWORDS: covalent organic frameworks, solid-state electrolytes, lithium-ion batteries, ion transport mechanisms, structure–property relationships

1 Introduction

Rechargeable batteries have played a foundational role in modern energy storage since the first secondary battery was introduced in 1860. The rapid growth of electrified transportation, portable electronics, and grid-scale storage has further intensified the demand for safe, high-energy, and durable battery systems [1–4]. Although lithium-ion batteries (LIBs) currently dominate the commercial market and continue to advance sustainable technologies, their liquid-electrolyte-based configuration faces inherent limitations that restrict further performance improvements [5–8]. Conventional liquid electrolytes (LEs), although offering high ionic conductivity and good interfacial wettability, suffer from flammability, leakage, volatility, and incompatibility with high-capacity anodes, particularly lithium metal [9–23]. These shortcomings lead to uneven Li^+ deposition,

Received: January 13, 2026; **Revised:** February 5, 2026
Accepted: February 12, 2026

✉Address correspondence to Dongli Xin, DongliXin@swjtu.edu.cn; Qi Kang, kangqi@sjtu.edu.cn or kangqi@swjtu.edu.cn; Lianbo Ma, mlb8976@ahut.edu.cn; Jie Xu, xu_jie@ahut.edu.cn

dendrite formation, potential separator penetration, and ultimately severe safety hazards such as internal short circuits, thermal runaway, and fires [24–32]. Moreover, the unstable solid electrolyte interphase (SEI) formed within the limited electrochemical window of LEs causes continuous electrolyte consumption, irreversible Li^+ loss, and reduced cycle life, all of which hinder energy density enhancement in next-generation rechargeable batteries [33–41].

To overcome these intrinsic drawbacks of liquid systems, research has increasingly focused on solid-state electrolytes (SSEs), a class of ion conductors that provide mechanical rigidity, nonflammability, broad electrochemical stability windows, and improved thermal robustness [42–45]. By physically inhibiting dendrite propagation and eliminating leakage- or combustion-related risks, SSEs address safety issues at their origin while enabling the practical deployment of lithium metal anodes [46–50]. As a result, tremendous progress has been made across inorganic ceramic SSEs (e.g., garnet, perovskite, NASICON, and sulfides) [51–58] and polymer-based electrolytes (e.g., polyethylene oxide (PEO), polyvinylidene difluoride (PVDF), and polyacrylonitrile (PAN)) [59–63]. However, each category faces persistent material challenges: Ceramics exhibit brittleness, high interfacial resistance, and poor processability, while polymer electrolytes often suffer from low room-temperature ionic conductivity, inadequate mechanical strength, or narrow electrochemical stability windows. These limitations collectively underscore the need for a new class of solid-state materials capable of uniting both fast ion transport and structural robustness.

Covalent organic frameworks (COFs), first reported by Yaghi and co-workers in 2005, have recently emerged as a highly promising platform to address these challenges [64, 65]. COFs are intricately synthesized through the covalent assembly of organic structural units characterized by precise symmetry, which bestows upon them the notable advantages of well-defined architectures, high porosity, and tunable nanopores [66–70]. Moreover, COFs empower researchers to meticulously manipulate the composition and architecture of crystalline and porous materials, intricately governing their periodic networks and the spatial arrangement of chemical functionalities (Fig. 1) [71]. In this process, the chemical structure and function of COFs can be meticulously tailored by programming backbone (Fig. 1(a)), incorporating functional groups (Fig. 1(b)), and chelating with specific ions (Fig. 1(c)) to generate a variety of COFs from two-dimensional (2D) to three-dimensional (3D) with controlled pore size, pore wall decoration, and stacking configurations (Figs. 1(d) and 1(e)) for energy applications.

Specially, the rigid covalent bonding in COFs endows excellent mechanical stability, while the ordered one-dimensional (1D) ion transport pathways enable low energy barriers for Li^+ migration (Fig. 2) [72–78]. Furthermore, the modularity of COFs allows for rational incorporation of functional groups, ion-conductive moieties, and hybridization strategies that are difficult to achieve in traditional inorganic or polymer electrolytes. These distinctive advantages offer exciting opportunities to engineer COF-based solid-state electrolytes that combine high conductivity, robust mechanical properties, and superior interfacial compatibility with lithium metal, features crucial for next-generation high-energy rechargeable batteries [79–81].

Given the rapid expansion of COF electrolyte research, a comprehensive assessment of their structural design principles, ion transport mechanisms, and practical challenges is both timely and necessary. This review aims to (i) elucidate the motivations for transitioning from liquid to solid electrolytes in advanced rechargeable batteries, (ii) summarize recent progress in COF-based SSEs across diverse structural categories, (iii) clarify the structure–transport–performance relationships underlying COF ion conduction, and (iv) provide critical insight into existing limitations and future directions. Beyond lithium metal batteries, we also highlight the emerging potential of COFs as solid-state ion conductors for other multivalent-ion storage systems. Through these discussions, we aim to offer a mechanistic and forward-looking perspective on the role of COFs in shaping the next era of solid-state rechargeable batteries.

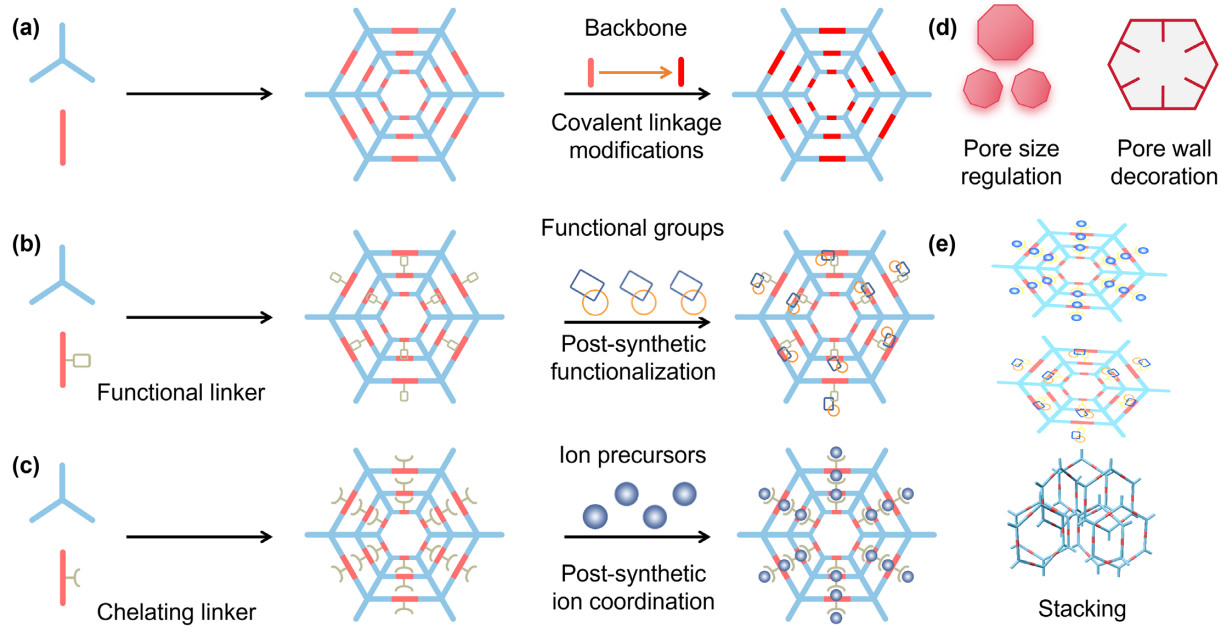

Figure 1 Diagram principle in the design of functional COFs for energy storage applications. (a) Covalent linkage modification, (b) functional groups modification, and (c) ionic precursors strategies for functional COFs with ((d) and (e)) controlled pore size, pore wall decoration, and diverse stacking configurations.

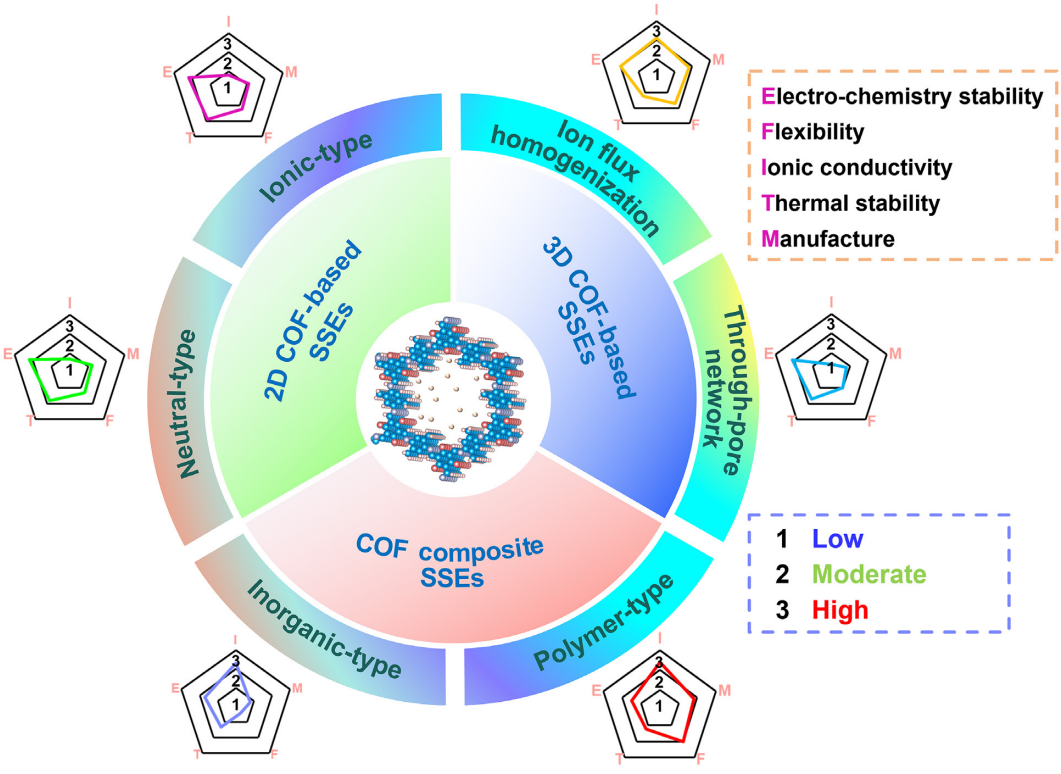

Figure 2 Illustration of the structural advantages and functionalization strategies of COFs for SSEs.

2 Emergence and rise of COF-based SSEs

The development of SSEs is driven by multiple technological demands and intrinsic limitations of conventional LEs. First, replacing flammable organic solvents with nonflammable solids fundamentally enhances the battery safety by eliminating the leakage and combustion risks. Second, SSEs can immobilize charge-compensating anions, thereby maximizing cation transference numbers and enabling more efficient Li^+ transport. Third, most LEs suffer from insufficient electrochemical stability windows, leading to side reactions with electrode materials; SSEs are designed to mitigate these parasitic processes and improve long-term cell stability [82]. In addition, their improved thermodynamic and electrochemical stability reduces byproduct formation and decreases the extent of SEI formation, ultimately increasing battery energy density by reducing the amount of excess cathode material needed to compensate for irreversible Li^+ loss [83]. For Li-metal anodes, where the dendrite formation remains a major challenge, LEs provide limited control over Li deposition morphology. By contrast, SSEs with adequate mechanical stiffness can homogenize Li nucleation, promoting uniform deposition/stripping and suppressing dendrite propagation [84–86].

COFs as emerging functional materials uniquely integrate the high structural order characteristic of inorganic solids with the tunability and functionality of organic polymers [87–90]. Owing to the synergy between crystalline precision and molecular designability, COF-based solid-state electrolytes have emerged as a promising class of solid-state ion conductors with significant potential for next-generation battery technologies [91–94]. Structurally, COFs are broadly classified into two categories, including 2D and 3D COFs depending on the geometry of their building blocks and connectivity patterns [71, 72, 95–105].

In 2D COFs, molecular building units link covalently within the *x*–*y* plane to form periodic layered architectures, while adjacent layers stack through π–π interactions to generate lamellar structures with well-aligned channels. Their relatively facile synthesis and wide monomer diversity have accelerated the rapid growth of 2D COF research in recent years [105–114]. In contrast, 3D COFs are constructed through tetrahedral linkages that propagate in three dimensions; however, their development remains comparatively limited due to restricted monomer availability and synthetic challenges [115–118]. Most 3D COFs are based on rigid aromatic motifs, while tetrahedral COFs typically incorporate sp^3-carbon or silicon nodes [119–123]. Their interconnected pore systems and elastic and dynamic frameworks can facilitate fast ion transport and offer advantages distinct from 2D analogues.

Recent advancements in COF-based SSEs have been considerable; key milestones are summarized in Fig. 3, illustrating both the evolution of COF materials and their expanding role in solid-state ion conduction. In 2D COFs, in-plane covalent bonding forms periodic polygonal pores, while π–π stacking between monolayers produces vertically aligned one-dimensional nanochannels along the *z*-axis [98, 103]. These continuous channels provide fast pathways for ion transport while maintaining high crystallinity and structural stability [124–128]. Similar to carbon nanotubes, graphene, and metal-organic frameworks (MOFs), COFs exploit nanoscale confinement effects within their channels to regulate molecular kinetics and thermodynamics [129, 130].

Although both MOFs and COFs employ ordered porous frameworks to enable ion transport, COFs possess several intrinsic advantages for solid-state battery applications. In contrast to MOFs built from heavy metal nodes and coordination bonds, COFs consist solely of light elements (C, H, O, N, and B) linked by robust covalent bonds, resulting in lower framework density and higher theoretical gravimetric energy density [131, 132]. Moreover, the

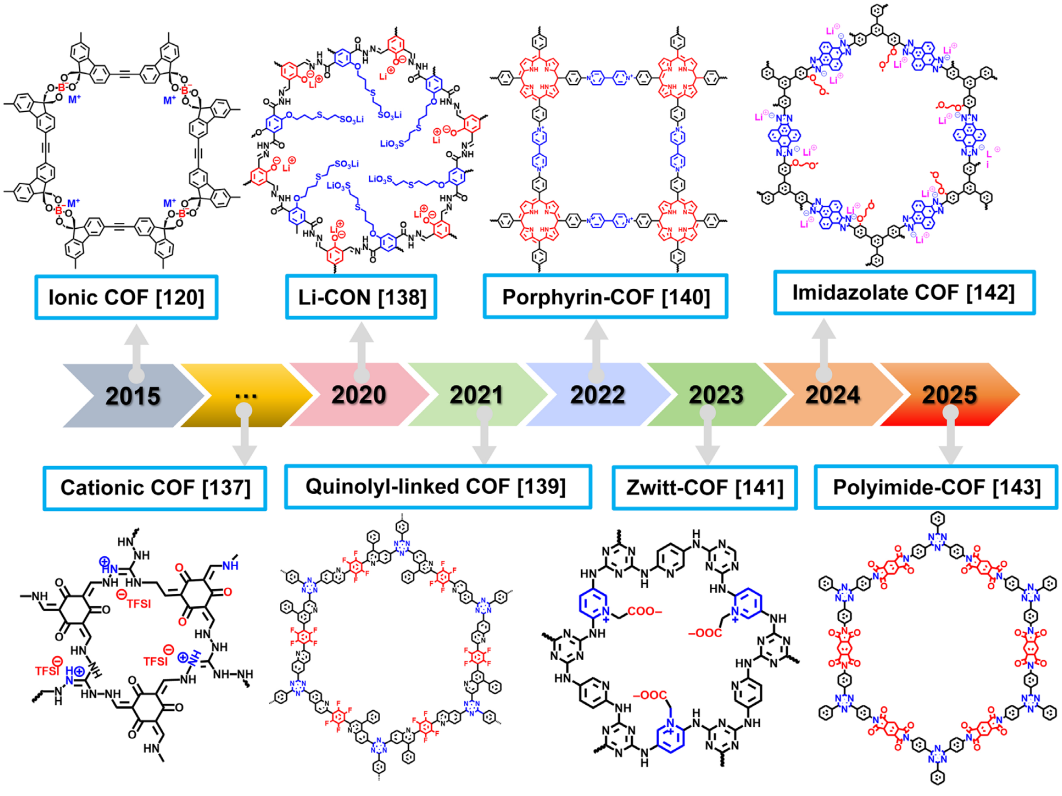

Figure 3 A brief chronology of the development of representative COF-based SSEs.

absence of redox-active metal centers in COFs eliminates the risk of metal-ion reduction at low potentials, an issue reported for some MOF-based electrolytes in contact with lithium metal anodes [133]. In addition, the rigid covalent backbone of COFs generally affords superior chemical and thermal stability compared to MOFs, ensuring structural integrity during prolonged cycling. These characteristics collectively establish COFs as a lightweight, electrochemically compatible, and structurally robust platform for next-generation solid-state electrolytes.

The development of 3D COFs is hindered by limited reversible bonding motifs and restricted topological diversity, mainly centered around tetrahedral (Td) building blocks such as tetraphenylmethane, tetraphenylsilane, tetraphenyladamantane, and various twisted monomers [120, 123, 134–136], which provide unique advantages in SSE design, including high surface area, large pore volume, abundant accessible sites, and multidirectional ion channels. These attributes offer new opportunities for tailoring ion transport and enhancing the performance of both LE- and SSE-based systems.

The high degree of synthetic designability further strengthens COFs' potential in SSE applications [137–152]. Their pore walls can be systematically functionalized through predesigned building blocks or post-synthetic modification strategies [74]. Such tunability enables COFs to: (1) form composite SSEs by physically incorporating inorganic electrolytes or chemically integrating ion-conductive polymers within neutral COF channels; (2) suppress anion migration through Lewis-acidic frameworks via acid–base interactions or through cationic skeletons via dielectric shielding; and (3) create anionic COFs by grafting lithiophilic Lewis-basic groups along pore walls to optimize the Li^+ conduction environment [79].

The ionic conductivity and transference numbers of representative COF-based SSEs are compiled in Table 1, highlighting their performance advantages compared with conventional solid polymer electrolytes (SPEs) and LEs. Table 1 summarizes the key performance metrics that are directly linked to practical battery requirements. Ionic conductivity is selected as the primary indicator of ion-transport efficiency, as sufficiently high values are essential to minimize ohmic polarization and support high-rate operation. Activation energy reflects the intrinsic barrier for ion hopping and is closely related to low-temperature performance. The Li^+ transference number evaluates ion-transport selectivity; values approaching unity are crucial for mitigating concentration polarization and suppressing dendrite formation, particularly in lithium metal batteries. The electrochemical stability window defines compatibility with high-voltage cathodes and thus limits the attainable energy density. Finally, Li|electrolyte|Li symmetric cell cycling performance provides a direct assessment of interfacial stability, dendrite suppression, and long-term operational reliability. Among these parameters, ionic conductivity constitutes the fundamental prerequisite for electrolyte feasibility, whereas the symmetric-cell cycling performance most closely reflects practical applicability by integrating interfacial, mechanical, and electrochemical factors.

3 Ion transport mechanisms in SSEs

The electrochemical performance of rechargeable batteries is intrinsically governed by ion/electron conduction within the electrolyte phase and across heterogeneous interfaces, namely the electrode–electrolyte boundary, the cathode–electrolyte interface (CEI), and the SEI. In conventional LEs, these transport processes arise from a dynamic and solvated environment, where the mobility of ions is aided by continuous solvent reorganization. In contrast,

Table 1 Summary of the electrochemistry performance of COF-based SSE

Electrolyte	Li//Li symmetric cells (plating current density (mA·cm^{-2})/cycling time (h))	Electrochemical window (V)	Transference number	Ionic conductivity	Activation energy (eV)	Ref.
CD-COF-Li	—	—	—	2.7×10^{-3} (30 °C)	0.26 (30 °C)	[123]
Li-CON-TFSI	—	3.8	0.61	5.74×10^{-5} (30 °C), 2.09×10^{-4} (70 °C)	0.34	[137]
Li-CON-1		4.5	0.86	2.13×10^{-4} (20 °C)	0.25	[138]
Li-CON-2		4.0	0.83	4.36×10^{-6} (20 °C)	0.22	[138]
Li-CON-3	0.05 + 0.1/500 (20 °C)	4.36	0.92	3.21×10^{-5} (20 °C) 0.9×10^{-5} (−40 °C)	0.13	[138]
Q-COF	0.1/1000 (60 °C) 0.2/800 (60 °C)	5.6	0.72	1.5×10^{-4} (60 °C)	0.15	[139]
COF-5/$LiClO_4$	—	—	—	2.6×10^{-4} (RT)	0.037 (RT)	[144]
TpPa-1/$LiClO_4$	—	—	—	1.5×10^{-4} (RT)	—	[144]
Ge-COF-1	—	—	—	1.0×10^{-5} (100 °C)	0.26 (100 °C)	[145]
Ge-COF-1/$LiPF_6$	—	—	0.67	3.5×10^{-3} (100 °C)	0.29 (100 °C)	[145]
COF-PEO-6	—	—	—	6.25×10^{-10} (30 °C) 7.94×10^{-6} (100 °C) 3.71×10^{-4} (200 °C)	—	[146]
COF-PEO-9		5.2		1.33×10^{-3} (200 °C)	—	[146]
TPB-DMTP-COF	—	—	0.96	1.36×10^{-7} (40 °C) 6.74×10^{-7} (60 °C) 5.37×10^{-6} (80 °C)	—	[147]
TPB-BMTP-COF	—	—	0.87	6.04×10^{-6} (40 °C) 2.85×10^{-5} (60 °C) 1.66×10^{-4} (80 °C) 5.49×10^{-4} (90 °C)	—	[147]
TpPa-SO_3Li	0.01/320	4.0	0.90	2.7×10^{-5} (RT)	0.18	[148]
Im-COF-TFSI@Li	0.02 + 0.1/300 (80 °C)	4.2	0.62	2.92×10^{-5} (30 °C)	0.32	[149]
dCOF-ImTFSI-60	0.02 + 0.1/300 (80 °C)	5.32	0.72	9.74×10^{-5} (30 °C)	0.28	[150]
H-Li-ImCOF	0.1/100	5	0.88	5.3×10^{-3} (RT)	0.13	[151]
CH_3-Li-ImCOF	—	4.5	0.93	8.0×10^{-5} (RT)	0.27	[151]
CF_3-Li-ImCOF	0.1/100	4.5	0.81	7.2×10^{-3} (RT)	0.1	[151]
PEG-Li^+@COF-M	0.4/2489 (100 °C)	5	—	2.2×10^{-5} (20 °C) 4×10^{-4} (80 °C)	0.46	[152]

SSEs eliminate liquid-phase mobility and instead rely on structurally constrained ionic migration, making ion transport fundamentally different and often rate-limiting.

COFs, with their crystallographically aligned 1D channels, tailorable pore surfaces, and rigid backbones, occupy a unique conceptual space between crystalline inorganic SSEs and amorphous polymer electrolytes. Their ordered nanochannels and chemically programmable pore walls endow them with the potential to support fast, selective, and tunable ion transport. Understanding these transport mechanisms is therefore essential for guiding the rational design of high-performance COF-based SSEs.

3.1 Ion transport in inorganic SSEs

In conventional LEs, ionic transport arises from three classical mechanisms: convection, diffusion, and electromigration. Among them, diffusion driven by concentration gradients dominates under open-circuit or weak polarization, whereas electromigration under an electric field becomes the primary transport mode during battery operation [82, 153]. Although these mechanisms ensure sufficient ion supply at reaction interfaces, they are intrinsically associated with liquid-phase drawbacks, including flammability, volatility, limited electrochemical stability, and inhomogeneous ion flux that promotes dendrite growth.

In inorganic SSEs, the absence of free solvent molecules

fundamentally changes the ion-transport landscape. Ionic motion occurs via thermally activated hopping through the rigid lattice, and is therefore strongly governed by crystallographic features and defect chemistry. The dominant transport carriers are structural defects, primarily Schottky defects (paired cation–anion vacancies) and Frenkel defects (cation vacancies coupled with interstitial cations) [150]. Materials rich in Frenkel defects generally exhibit lower activation energies and higher ionic conductivities, as interstitial ions migrate more readily than vacancy-bound species [154]. In addition, intrinsic ion properties (such as valence state, ionic radius, and charge density) critically influence migration barriers: Higher valence ions experience stronger electrostatic binding, while excessively large or small ions suffer from steric constraints or trapping effects, respectively.

3.2 Ion transport in polymer-based SSEs

In polymer-based solid-state electrolytes, ion transport is intimately coupled to polymer chain dynamics. Above the glass transition temperature (T_g), segmental motion of polymer chains creates transient coordination sites that enable metal ions to hop between neighboring electronegative groups, such as ether oxygens, nitriles, carbonyls, or fluorinated moieties along the backbone [82, 91, 155, 156]. This transport process involves continuous coordination–dissociation events and is therefore intrinsically limited by the rate of polymer segmental relaxation.

Such coupling gives rise to a fundamental trade-off between ionic conductivity and mechanical stability. Enhancing chain mobility by reducing crystallinity or softening the polymer matrix facilitates ion transport but compromises mechanical strength, whereas reinforcing the polymer backbone suppresses deformation at the expense of ionic mobility. Consequently, many polymer electrolytes exhibit insufficient room-temperature ionic conductivity ($< 10^{-5}$–10^{-4} S·cm^{-1}), particularly when crystallization or chain confinement becomes pronounced.

To mitigate this limitation, strategies including plasticization, single-ion conducting polymers, ceramic fillers, and block copolymer architectures have been explored. However, these approaches often introduce additional challenges related to phase separation, interfacial compatibility, and long-term durability. The intrinsic dependence of ion transport on polymer dynamics thus remains a key bottleneck for polymer-based SSEs in high-energy solid-state batteries.

3.3 Ion transport in COF-based SSEs

Compared with inorganic ceramic electrolytes, COF-based solid-state electrolytes exhibit markedly superior mechanical flexibility and interfacial compliance. In particular, polymer-COF composite films and quasi-solid COF architectures can be processed into ultrathin and mechanically robust membranes that maintain high ionic conductivity under repeated bending, twisting, or folding, making them attractive for flexible, wearable, and shape-conformal energy storage devices. Moreover, the structural compliance of COF frameworks (especially when coupled with soft polymeric or gel phases) enables effective accommodation of electrode volume changes during cycling. This mechanical buffering preserves intimate electrode–electrolyte contact, mitigates interfacial stress accumulation, and suppresses delamination or fracture, thereby enhancing the long-term cycling stability of solid-state batteries relative to rigid ceramic systems.

COFs constitute a structurally unique class of SSEs whose ion transport behavior extends beyond the classical descriptions established for crystalline ceramics and polymeric electrolytes. Their periodic lattices, tunable pore architectures, and chemically designable skeletons give rise to multiple, often coexisting, ion conduction pathways that can be tailored with molecular-level precision. This combination of crystallinity and synthetic programmability enables COFs to bridge the gap between rigid inorganic SSEs and flexible polymer matrices, offering a versatile platform for fast and selective ion migration.

First, crystallographically aligned 1D nanochannels arising from the π–π stacking of 2D COF layers, which provide straight, continuous, and low-tortuosity pathways for cation transport. These vertically oriented channels minimize scattering events and suppress the bottlenecks commonly observed in amorphous polymer systems, allowing ions to traverse long distances through a structurally coherent framework. Second, the high mechanical rigidity and thermal/chemical robustness bestowed by fully covalent bonding ensure that these conduction pathways remain intact during cycling, preventing channel collapse or pore deformation, which are major limitations in polymer SSEs.

A distinct advantage of COFs lies in their programmable pore surface chemistry. By decorating pore walls with Lewis acidic or Lewis basic groups, constructing cationic or anionic frameworks, or incorporating solvating moieties, the local coordination environment can be precisely tuned to regulate ion binding strength, desolvation behavior, and hopping frequency. These design features directly reshape the free-energy profile of ion migration within COF pores. Furthermore, the nanoconfinement effect inherent to ordered COF channels modulates the ion solvation structure, often reducing solvation shell size, altering coordination numbers, and weakening ion–solvent interactions, which collectively lower the activation barrier for migration.

Depending on chemistry and spatial configuration, COFs can support hybrid ion transport mechanisms, including vacancy-like hopping reminiscent of crystalline SSEs, coordination–dissociation processes similar to polymer electrolytes, or the migration of confined liquid-like ion species along pore interiors. Such coexistence of distinct transport modes is rarely attainable in traditional SSEs, enabling COFs to simultaneously achieve fast ion conduction, high electrochemical stability, and tunable ion selectivity.

Altogether, the structural precision and functional modularity of COFs offer unprecedented opportunities to engineer SSEs with tailored conduction pathways, positioning them as a compelling platform for next-generation solid-state battery technologies.

4 Classification of COF-based solid electrolytes

The rigid covalent backbones of COFs endow COF-based solid-state electrolytes with excellent thermal stability, often preserving structural integrity at temperatures exceeding 300 °C. Such robustness allows the electrolyte to remain mechanically and chemically intact under thermal abuse, thereby maintaining effective electrode separation. More importantly, replacing flammable liquid electrolytes with non-volatile solid or quasi-solid COF architectures removes the primary combustible component from the cell, interrupting the heat–fuel feedback loop that drives thermal runaway. As a result, COF-based electrolytes offer intrinsic advantages in mitigating thermal runaway and enhancing battery-level safety.

COFs have emerged as a promising class of porous crystalline SSEs due to their rigid and thermally stable backbones and periodically ordered channels, which together offer well-defined spaces for accommodating lithium salts and constructing efficient ion-transport pathways [135, 157]. The intrinsic tunability of their pore environments through tailored functional groups or charged building units further facilitates lithium salt dissociation at specific coordination sites and promotes directional Li^+ migration. These structural merits position COFs as a distinctive platform for engineering solid electrolytes with programmable conduction behavior.

Despite their unique advantages, the practical deployment of COF-based electrolytes in all-solid-state lithium batteries (ASSLBs) still encounters substantial challenges. Compared with established inorganic and polymer SSEs, the overall ionic conductivity of COF-based systems generally remains below the threshold required for commercial operation, particularly under ambient conditions [158].

From the perspective of framework charge characteristics (a key parameter influencing ion distribution, salt dissociation, and migration behavior), COF-based SSEs can be broadly classified into neutral COFs and ionic COFs. The latter can be further divided into cationic and anionic frameworks, each exhibiting distinct interactions with Li^+ and counterions, thereby supporting different conduction modes and design strategies.

4.1 Neutral COFs

2D neutral COFs, formed by covalent assembly of organic linkers into periodic frameworks, possess ordered nanopores, adjustable backbone functionality, and a balance of polymer-like flexibility with inorganic-level mechanical rigidity. These features make them promising candidates for SSEs capable of facilitating directional ion transport.

Vazquez-Molina et al. demonstrated that mechanically pressed COF powders form thin and highly anisotropic pellets, enabling detailed investigation of crystallographic orientation and ion conduction pathways [144]. X-ray diffraction (XRD) analysis revealed that 2D layers lie in the *ab*-plane and stack along the *c*-axis via π–π interactions, producing orthogonal (*hk*0) and (00*l*) reflections (Fig. 4(a)). This pressing strategy was shown to be compatible with multiple COF chemistries including boronic esters, boroxanes, β-ketoenamines, and triazines with both hexagonal and tetragonal symmetries (Fig. 4(b)). Pressed COF-5 transformed from spherical powders into lamellar structures whose vertically aligned pores act as straight channels for Li^+ migration (Fig. 4(c)).

Solid-state ^7Li nuclear magnetic resonance (NMR) further confirmed enhanced ion mobility: $LiClO_4$ confined within COF-5 displayed a signal nearly four orders of magnitude shorter in relaxation time than pure $LiClO_4$ powder, evidencing rapid internal Li^+ motion and migration through the 1D pores (Fig. 4(d)). Although these results highlight the potential of 2D COFs as solid electrolytes, the detailed migration mechanism within confined channels requires deeper understanding.

To probe this, Pan et al. performed molecular dynamics (MD) simulations on COF-5 filled with tetrahydrofuran (THF)/$LiClO_4$ [135]. Li^+ was found to migrate in a liquid-like manner, solvated by THF and undergoing continuous coordination–dissociation with

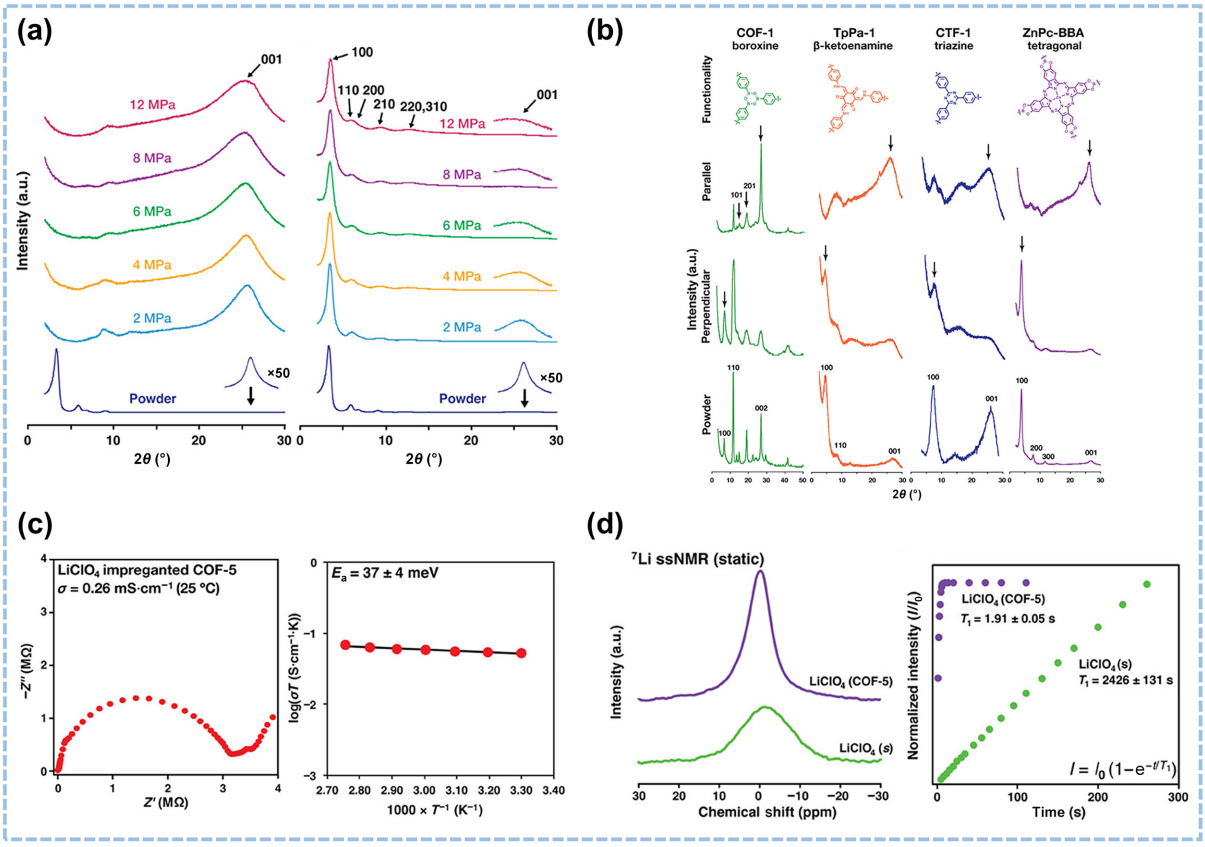

Figure 4 (a) PXRD patterns of a COF-5 pellet with varying uniaxial pressure. (b) PXRD patterns of COF pellet oriented perpendicular to the optical axis. (c) Nyquist plots of and Arrhenius plot of COF-5 impregnated with $LiClO_4$. (d) ^7Li magic angle spinning (MAS) NMR spectra of COF-5 impregnated with $LiClO_4$ and compared to pure $LiClO_4$ and Saturation recovery plot from ^7Li MAS NMR. Reproduced with permission from Ref. [144], © American Chemical Society 2016.

ClO_4^- and THF oxygen atoms (Fig. 5(a)). The framework confines anions and solvent, modulating rotational motion while allowing Li^+ to move longitudinally along the channel. Their results suggest that optimizing pore size and matching it with salt ion size can enhance conductivity, whereas excessive salt concentration slows Li^+ transport (Fig. 5(b)). These insights provide guidance for tuning pore dimensions and solvent/salt ratios in future high-performance 2D-COF SSEs.

A major limitation of earlier neutral COF SSEs lies in their thickness (> 100 μm) and use of dynamic imine linkages, which, despite improved crystallinity, compromise chemical and electrochemical stability for high-energy lithium metal batteries. To address this, Xu et al. converted imine-linked I-COFs with triazine and polyfluorophenyl groups into more robust quinoline-linked Q-COFs through a Povarov reaction (Fig. 5(c)) [139]. MD simulations revealed that Li^+ primarily coordinates with triazine and polyfluorophenyl groups, while excess Li^+ occupies the channel center. RDF analysis (Fig. 5(d)) showed Li–O ($TFSI^-$) distances of ~ 0.2 nm and Li–N distances of ~ 0.5 nm, indicating a coordination–dissociation–assisted migration mechanism within the 1D channels.

Mechanically pressed Q-COF films displayed strong (001)-orientation, substantially boosting ionic conductivity. The resulting Li/Q-COF SSE/NMC811 cell delivered excellent cycling stability and high Coulombic efficiency (CE) and the Q-COF SSE was further validated in flexible pouch-cell demonstrations. These advances highlight the potential of stabilized neutral COFs to overcome the traditional limitations of imine-based systems and enable thinner and high-voltage-compatible solid-state electrolytes.

4.2 Cationic COFs

Ionic conductivity in solid electrolytes depends on both the concentration of free Li^+ and its mobility. In traditional liquid and polymer electrolytes, strong Coulombic interactions promote ion pairing or clustering, severely hindering Li^+ transport and accelerating capacity fade. Accordingly, recent strategies to enhance conductivity largely focus on increasing free Li^+ concentration by immobilizing anions or suppressing their migration through electrostatic shielding [123]. COFs offer additional advantages because their functional groups and ordered pore frameworks can modulate Lewis acid–base interactions and dielectric environments to facilitate lithium salt dissociation [159].

A pioneering example appeared in 2015, when Zhang et al. designed ionic COFs (ICOFs) containing sp^3-hybridized boron anionic centers with tunable countercations [120]. These ICOFs exhibited excellent chemical and thermal stability and incorporated fixed ionic sites capable of supporting Li^+ conduction. The reported room-temperature ionic conductivity (3.05×10^{-5} S·cm^{-1}) and high Li^+ transference number (0.80 ± 0.02) highlighted the promise of ionic frameworks for next-generation SSEs. Based on their charge characteristics, ICOFs can be categorized as either cationic or anionic.

Cationic COFs have attracted particular attention due to their ability to promote lithium salt dissociation and suppress ion agglomeration, longstanding obstacles for solid electrolytes. Chen et al. [137] developed a cationic COF electrolyte (Li-CON-TFSI) that integrates three synergistic mechanisms (Figs. 6(a)–6(c)): (i) The positively charged framework enhances the dielectric constant, weakening Coulombic interactions and reducing ion pairing; (ii) the polarized skeleton strengthens electrostatic attraction toward anions, further limiting their mobility; and (iii) abundant carbonyl oxygen atoms create Li^+–O coordination sites that improve Li^+ mobility. As a result, Li-CON-TFSI achieved a Li^+ conductivity of 2.09×10^{-4} S·cm^{-1} at 70 °C, with ^{7}Li NMR and Fourier transform infrared (FTIR) confirming enhanced ion-pair dissociation (Figs. 6(d) and 6(e)).

Insights from polymerized ionic liquids (PILs) further motivate the design of COF-based ionic conductors. Imidazolium-containing PILs typically outperform other cationic polymers, and $TFSI^-$ consistently yields higher conductivity than BF_4^- or PF_6^- due to its hydrophobicity and limited coordination sites [149]. COFs with tunable pore structures provide an excellent platform to integrate these favorable ionic units.

Following this rationale, Feng et al. synthesized an imidazolium-functionalized COF (Im-COF-Br), subsequently exchanged with $TFSI^-$ to obtain Im-COF-TFSI (Fig. 7(a)) [149]. Blending with lithium bis(trifluoromethanesulfonyl)imide (LiTFSI) produced Im-COF-TFSI@Li, which exhibited substantially higher ionic

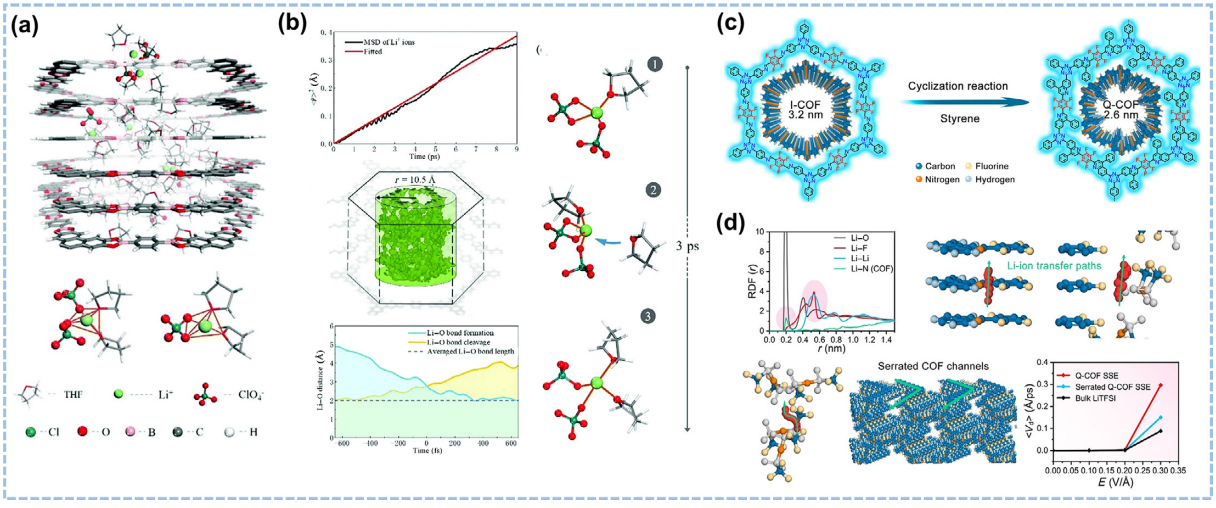

Figure 5 (a) The schematic of 1D Li^+ transfer paths of 2D-COF filled with Li salt and solvent. (b) AIMD simulation of Li^+ diffusion. Reproduced with permission from Ref. [135], © The Owner Societies 2019. (c) Synthetic scheme of Q-COF. (d) Radial distribution functions LiTFSI in the Q-COF, three representative Li^+ diffusion routes, serrated model of Q-COF layers with AA fashion, and Li^+ diffusion rate of three environments under an external electric field. Reproduced with permission from Ref. [139], © Wiley-VCH GmbH 2021.

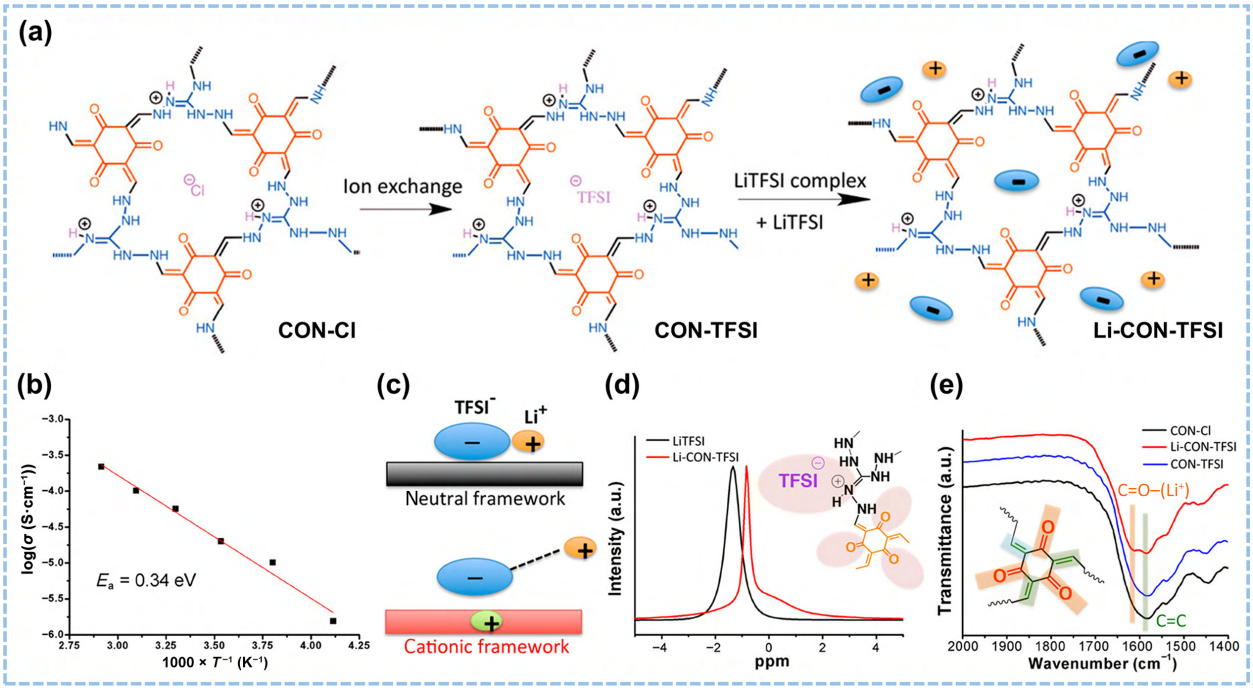

Figure 6 (a) Synthesis route of the cationic covalent organic framework nanosheets. (b) Arrhenius plot of LiCON-TFSI ionic conductivity with different temperatures. (c) The schematic of the ion pair around cationic framework. (d) ^{7}Li MAS NMR spectra of LiTFSI and Li-CON-TFSI. (e) FTIR spectra of CONs, COF-TFSI, and LiCON-TFSI. Reproduced with permission from Ref. [137], © American Chemical Society 2018.

conductivity than neutral COFs or the bromide analogue, reaching 2.92×10^{-5}, 4.64×10^{-5}, and 4.64×10^{-3} S·cm^{-1} at 303, 353, and 423 K, respectively (Fig. 7(b)). Symmetric Li/Im-COF-TFSI@Li/Li cells delivered low polarization and stable interfaces, and full Li/Im-COF-TFSI@Li/LFP cells showed a capacity retention of 91.6% after 100 cycles with a CE of ~ 98%.

Beyond framework charge design, defect engineering has recently emerged as a powerful means to enhance ionic COFs. Han et al. employed a three-component condensation reaction to generate defective 2D COFs (dCOFs) containing unreacted aldehyde or amine anchoring sites (Fig. 7(c)) [150]. Post-synthetic grafting of imidazolium cations followed by $TFSI^-$ exchange incorporated high densities of mobile ionic species within the channel walls. The optimized electrolyte, dCOF-ImTFSI-60@Li, achieved a record Li^+ conductivity of 7.05×10^{-3} S·cm^{-1} at 423 K, among the highest reported for crystalline porous polymer electrolytes, and enabled stable cycling in Li|dCOF-ImTFSI-60@Li|LFP cells across 303–423 K.

Collectively, cationic COFs leverage electrostatic shielding, Lewis acid–base interactions, and pore-confined anion regulation to suppress ion aggregation and release highly mobile Li^+. Their modular structures and tunable ionic environments provide a versatile platform not only for Li^+ but potentially for Na^+, K^+, Mg^{2+}, and Al^{3+} SSEs.

4.3 Anionic COFs

Anionic COFs have emerged as an effective strategy to overcome the inherent limitation of conventional salt-in-COF systems, in which freely migrating anions hinder the Li^+ transport and depress the Li^+ transference number. By covalently incorporating weakly coordinating anionic groups, such as boronate, imidazolate, carboxylate, sulfonate, or sulfonimide, into the COF framework, researchers have realized materials in which only Li^+ serves as the mobile carrier while the anions remain immobilized within the backbone [87, 148, 152, 160–162]. This architectural principle not only eliminates anion-related polarization but also maintains the mechanical robustness of the porous scaffold.

Imidazolate-functionalized COFs represent a representative example of such single-ion conductors. Owing to the weak binding affinity between imidazolate anions and Li^+, the anions remain tethered while Li^+ migrates through the ordered channels. Based on this concept, Zhang et al. developed a series of imidazolyl ionic COFs (Li-ImCOFs) using a bottom-up synthetic approach (Fig. 8(a)) [151]. Systematic modification of the imidazole linker by introducing H, CH_3, or CF_3 substituents revealed that electron-withdrawing groups (particularly CF_3) effectively delocalize the anionic charge, thereby weakening Li^+–framework interactions and accelerating Li^+ hopping. The conductivity trends clearly follow this electronic modulation (Fig. 8(b)), underscoring the tunability of imidazolate COFs as a platform for exclusive Li^+ transport and stable electrochemical operation.

Despite these advances, partial detachment of grafted anions or the presence of trace solvent within COF pores may still trigger parasitic reactions at Li metal surfaces, generating concentration gradients that promote dendrite formation. Addressing this challenge requires truly solvent-free frameworks with fully immobilized anions. Lee et al. introduced a benchmark material in this direction, TpPa-SO_3H, featuring covalently embedded sulfonate groups that, after ion exchange to form TpPa-SO_3Li, provide solvent-free, sub-nanometre, and single-ion-conducting channels (Fig. 8(c)) [148]. Density-functional theory calculations reveal strongly anisotropic transport, with a markedly lower axial migration barrier (7.6 kcal·mol^{-1}) relative to the planar direction (31.6 kcal·mol^{-1}). Li^+ diffusion proceeds via coordinated hopping between sulfonate and keto oxygen atoms, stabilized by cation–dipole interactions. Symmetric Li|TpPa-SO_3Li|Li cells show low and stable interfacial resistance, while post-cycling analyses

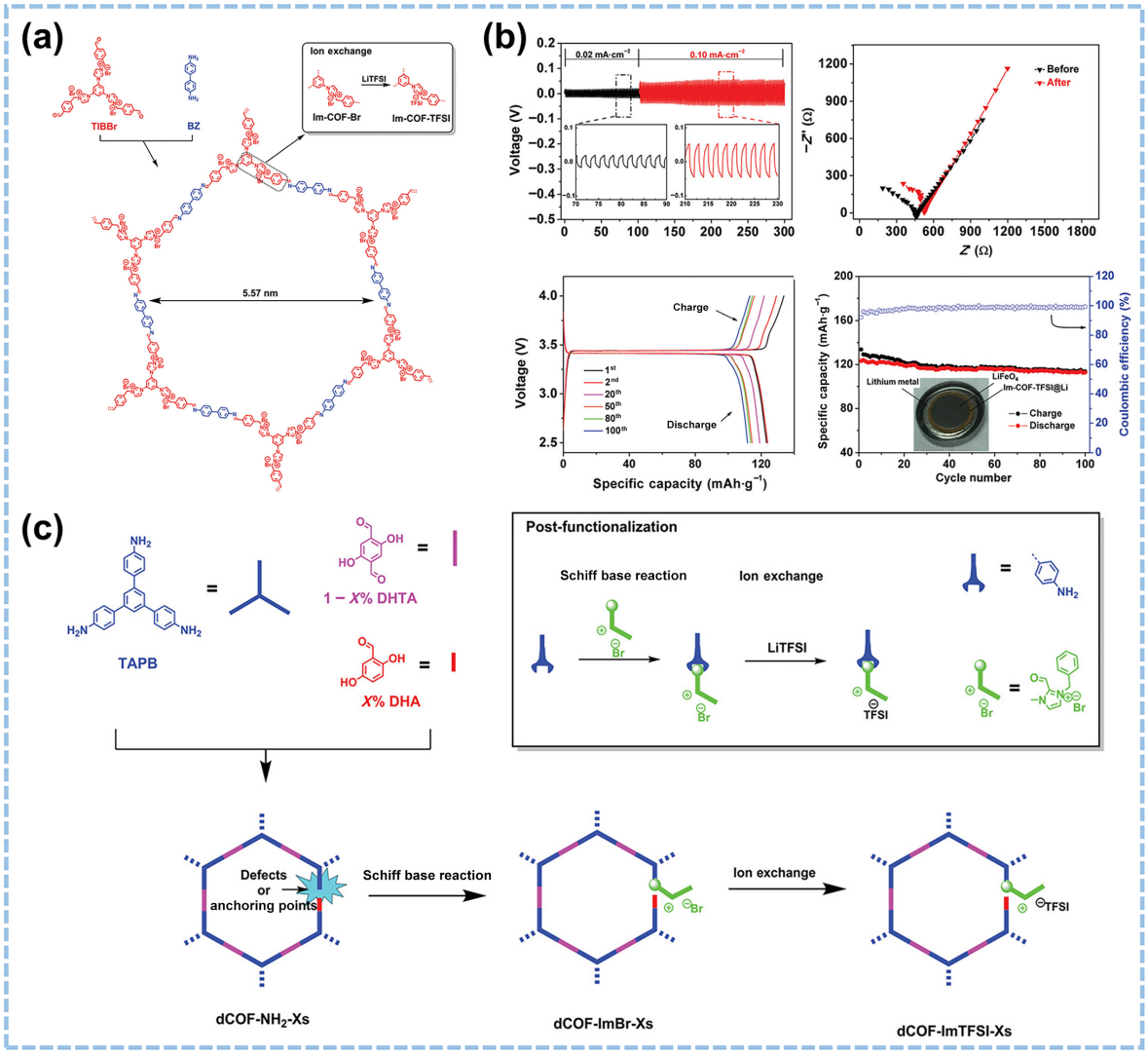

Figure 7 (a) Synthetic scheme of Im-COF-Br and Im-COF-TFSI. (b) Electrochemical performances of Im-COF-TFSI SSEs. Reproduced with permission from Ref. [149], © The Partner Organisations 2020. (c) Synthesis route of dCOF-NH_2-Xs, dCOF-ImBr, and dCOF-ImTFSI. Reproduced with permission from Ref. [150], © WILEY-VCH Verlag GmbH & Co. KGaA, Weinheim 2020.

confirm smooth and dendrite-free lithium deposits (Fig. 8(d)). Eliminating both mobile anions and residual solvent thus ensures uniform flux and greatly suppresses interfacial instability.

The generality of this design principle extends beyond Li^+. The TpPa-SO_3M platform can be exchanged with Na^+, K^+, Mg^{2+}, Ca^{2+}, Zn^{2+}, or Al^{3+}, providing a versatile class of solvent-free single-ion conductors adaptable to diverse metal battery chemistries.

In addition to sulfonate-based systems, post-synthetically modified hydrazone-linked COFs offer another route toward tunable anionic frameworks. Loh et al. [138] grafted thioether-tethered acidic or ionic groups onto phenol-containing COFs via thiol-ene click chemistry, followed by lithiation to generate phenolate anions that promote spontaneous exfoliation into covalent organic nanosheets (CONs) (Fig. 9(a)). The resulting LiCON-1/2/3 materials exhibit high Li^+ transference numbers, with LiCON-3 achieving 10^{-5} S·cm^{-1} and t_{Li^+} of 0.92 at −40 °C. Paired with a 1,4-benzoquinone cathode, the corresponding solid-state battery retained stable cycling over 500 cycles at 500 mA·g^{-1} and 20 °C, demonstrating the robustness and scalability of this modular COF platform.

Building on these concepts, Guo et al. [161] designed acetate-functionalized COFs (LiOOC-COF1/2/3) in which lithiated carboxylates enhance Li^+ transport, reduce polarization, and improve interfacial compatibility, mechanistically akin to sulfonate systems (Fig. 9(b)). A bis-lithium sulfonate analogue, Li_2O_3S-COF2, further delivers a conductivity of 5.47×10^{-5} S·cm^{-1} and a Li^+ transference number of 0.93 at ambient temperature. In all cases, exfoliation into ultrathin nanosheets markedly increases accessible diffusion pathways, elevating ion-transport kinetics.

Overall, anionic COFs through rational anchoring of weakly coordinating anions, solvent-free processing, and nanosheet engineering have significantly advanced the development of single-ion SSEs. These achievements not only improve the performance of Li-based SSEs but also chart a clear path toward extending COF-based single-ion conductors to a wider range of multivalent metal-ion systems.

5 COF-based composite SSEs

Despite the significant progress achieved with COF-only SSEs, their room-temperature ionic conductivity still falls short of practical

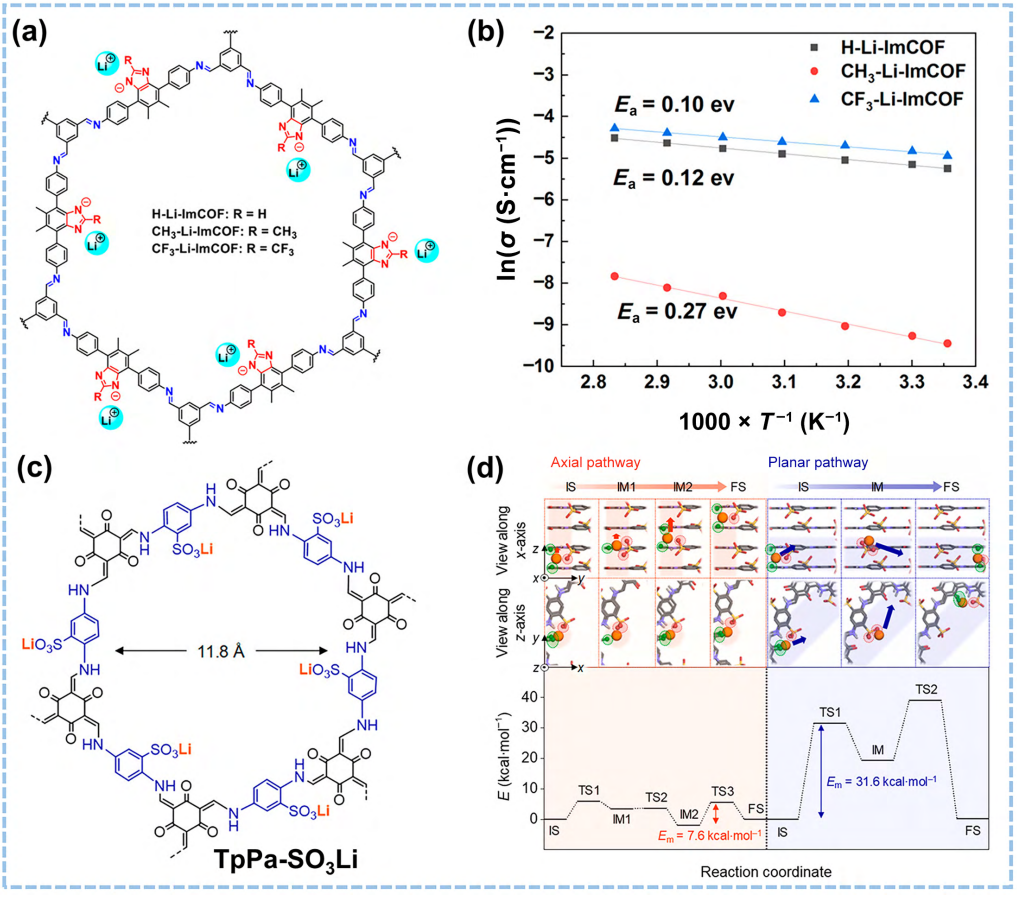

Figure 8 (a) Chemical structure of R-ImCOFs. (b) Arrhenius plot of ionic conductivity of H-Li-ImCOF, CH_3-Li-ImCOF, and CF_3-Li-ImCOF under varing temperature. Reproduced with permission from Ref. [151], © American Chemical Society 2019. (c) Chemical structure of sulfonated COF (TpPa-SO_3Li), (d) Theoretical elucidation of Li^+ migration behaviors. Reproduced with permission from Ref. [148], © American Chemical Society 2019.

requirements for commercial solid-state LIBs. To bridge this gap, hybridizing COFs with inorganic or polymeric matrices has become an increasingly attractive route, as such composites can leverage the structural merits of COFs while compensating for their intrinsic transport limitations.

Polymer gels with 3D and cross-linked networks swollen by compatible solvents provide a representative example of how composite strategies can enhance ion conduction. Their solvent-philic domains immobilize liquid phases within a flexible framework, enabling molecular-level structural control [93]. Owing to their nonvolatility, leak-free operation, facile processability, and environmental friendliness, gel polymer electrolytes (GPEs) have been widely adopted in electrochemical energy storage [163–168]. However, the amorphous and structurally disordered nature of traditional GPEs hinders clear structure–property correlations, limiting targeted optimization.

COFs offer the opposite advantage: crystalline order with precisely defined pore environmen [169, 170]. Yet, their high melting points, strong solvent/acid resistance, and powdery form constrain their direct processability [93, 171]. Although thin COF films or membranes can be obtained through chemical or mechanical routes, these products typically suffer from fragility, low surface area, and poor yield [152]. Embedding COFs into gel architectures therefore represents a promising strategy that simultaneously preserves crystallinity and enables practical fabrication.

To this end, Zhang et al. proposed a bottom-up gelation strategy inspired by MOF research [172]. By integrating branched alkyl side chains during synthesis, COF layers are partially decoupled, allowing solvent uptake at room temperature (RT) and inducing a controlled "powder-gel" transition (Fig. 10(a)). Adjusting the length of these side chains enables fine regulation of morphology, ultimately yielding transparent, mechanically stable, free-standing COF-Gels (Fig. 10(b)). These gels retain the chemical robustness of COFs while gaining the flexibility and processability required for device integration.

When applied as solid electrolytes, COF-Gels deliver impressive performance. Li|COF-Gel|$LiFePO_4$ cells exhibit stable cycling over 1200 cycles at 5 C with minimal capacity decay, outperforming analogous liquid-electrolyte systems (Figs. 10(c) and 10(d)). This work underscores the potential of COF-based gel architectures: Not only do they reconcile crystallinity with mechanical compliance, but they also illustrate how rational molecular design can extend into the gel state, enriching the scope of COF-derived SSEs and offering new opportunities for crystal-engineering strategies (Fig. 10(e)).

5.1 Inorganic-type COF composite

Inorganic SSEs have achieved major breakthroughs in recent years, with garnet-type materials standing out due to their high room-temperature Li^+ conductivity (~ 1 mS·cm^{-1}) and excellent chemical robustness [173]. However, their practical deployment is hindered by severe interfacial instability with Li metal. Although several

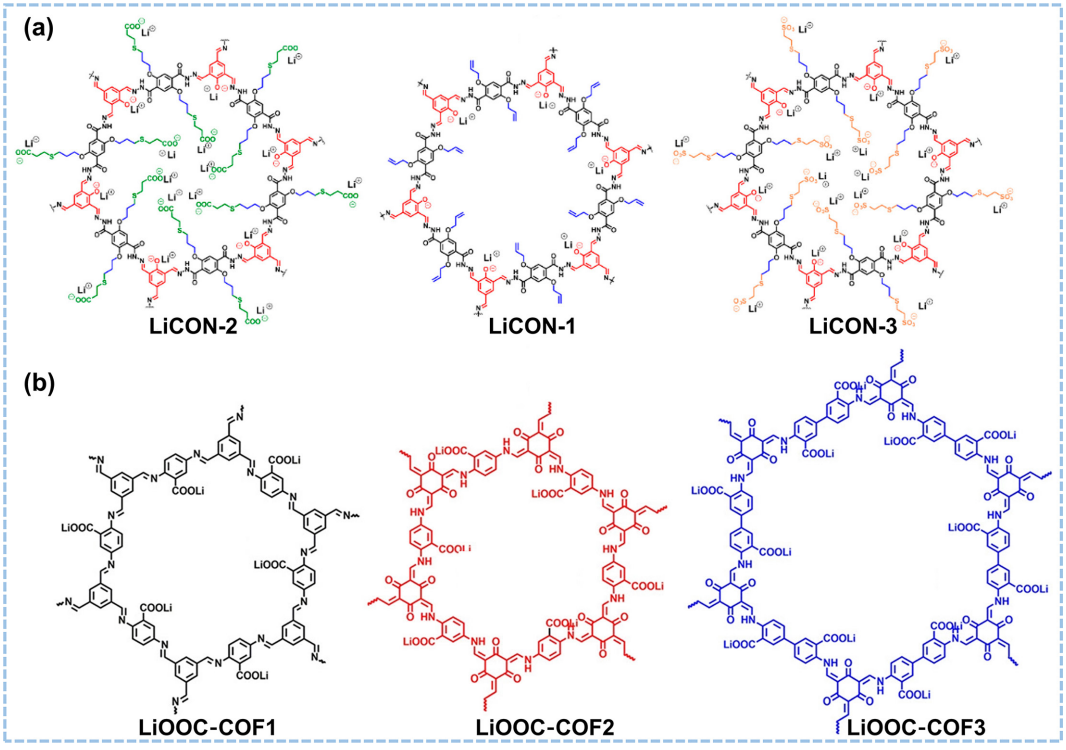

Figure 9 Chemical structure of (a) lithium sulfonated CONs. Reproduced with permission from Ref. [138], © American Chemical Society 2020. (b) lithium acetate COFs. Reproduced with permission from Ref. [161], © Zhao, G. F. et al. 2022.

surface treatments have been explored, their complexity and limited compatibility have slowed wider adoption [174].

COFs offer a complementary set of advantages: intrinsically stable interfaces with Li metal (Li^+ transference number ≈ 0.9), tunable pore environments, and moderate ionic conductivity (up to 2.7×10^{-5} S·cm^{-1} at ambient temperature). More importantly, COFs can be grown as uniform and ultrathin films on diverse substrates through mild solution processes serving as an attractive feature for engineering well-defined inorganic–organic heterointerfaces in SSLBs.

Leveraging this, Chen et al. [173] fabricated a sulfonated COF interlayer (csCOF@LLZTO) directly on the surface of $Li_{6.4}La_3Zr_{1.4}Ta_{0.6}O_{12}$ (LLZTO) via room-temperature *in-situ* solution growth (Fig. 10(f)). The resulting sub-500 nm coating forms a dense Li^+-conducting interphase between LLZTO and Li metal. Upon curing, the amorphous precursor reorganizes into an ordered COF, further facilitating ion transport (Fig. 10(g)). This modification sharply reduces interfacial resistance from 908 to 99 Ω·cm^2 and greatly stabilizes the Li/garnet interface. As a result, Li|csCOF@LLZTO|Li symmetric cells operate stably at 3 mA·cm^{-2}, while Li|c*sCOF@LLZTO|$LiFePO_4$ full cells deliver strong rate capability at 2 C (Fig. 10(h)).

Although promising, this approach remains in its early stages. The broader applicability of *in-situ* COF interlayers across different garnet compositions, cell architectures, and scalable processing routes warrants further investigation.

5.2 Polymer-type COF composite

Although inorganic SSEs continue to advance, polymer-based counterparts remain indispensable owing to their mechanical flexibility and interfacial compatibility. PEO has long served as the archetype polymer electrolyte due to its facile processability, high salt-solvation capability, and compatibility with high-energy-density LIBs. However, its strong crystallinity at room temperature severely restricts segmental motion, leading to intrinsically low ionic conductivity and preventing reliable ambient-temperature operation [146, 147, 175].

A variety of modifications including PEO grafting, copolymerization, and extensive cross-linking have attempted to mitigate this limitation, yet none has successfully produced continuous, fast Li^+ transport pathways. Quasi-solid approaches, where liquid electrolytes are imbibed into porous hosts, temporarily enhance conductivity but reintroduce leakage and safety risks. Meanwhile, COFs offer ordered 1D channels that could, in theory, direct ion migration; however, simple pore loading of lithium salts via solvent infiltration yields conductivities far below practical thresholds.

To overcome this bottleneck, Jiang et al. [147] engineered a polyelectrolyte COF (Li^+-PEO_{400}@TPB-DMTP-COF) in which short oligo(ethylene oxide) chains are covalently grafted onto pore walls (Fig. 11(a)). Complexation with Li^+ forms a continuous polyelectrolyte interface within the rigid framework, combining COF structural order with the solvating ability of PEO. This hybrid design boosts ionic conductivity by over three orders of magnitude relative to the pristine COF while maintaining thermal robustness and enabling a vehicle-type transport mechanism (Fig. 11(b)). By integrating flexible polymer segments into crystalline nanochannels, this strategy provides a clear blueprint for constructing polymer–COF hybrid transport pathways.

Manthiram et al. [164] advanced a complementary approach by embedding a solvent–salt pair (dimethylacrylamide (DMA)/LiTFSI) directly into COF nanochannels. In this solvent-in-pore configuration (DMA@LiTFSI-mediated COF (DLC)), flexible DMA molecules act as internal plasticizers, weakening Li^+

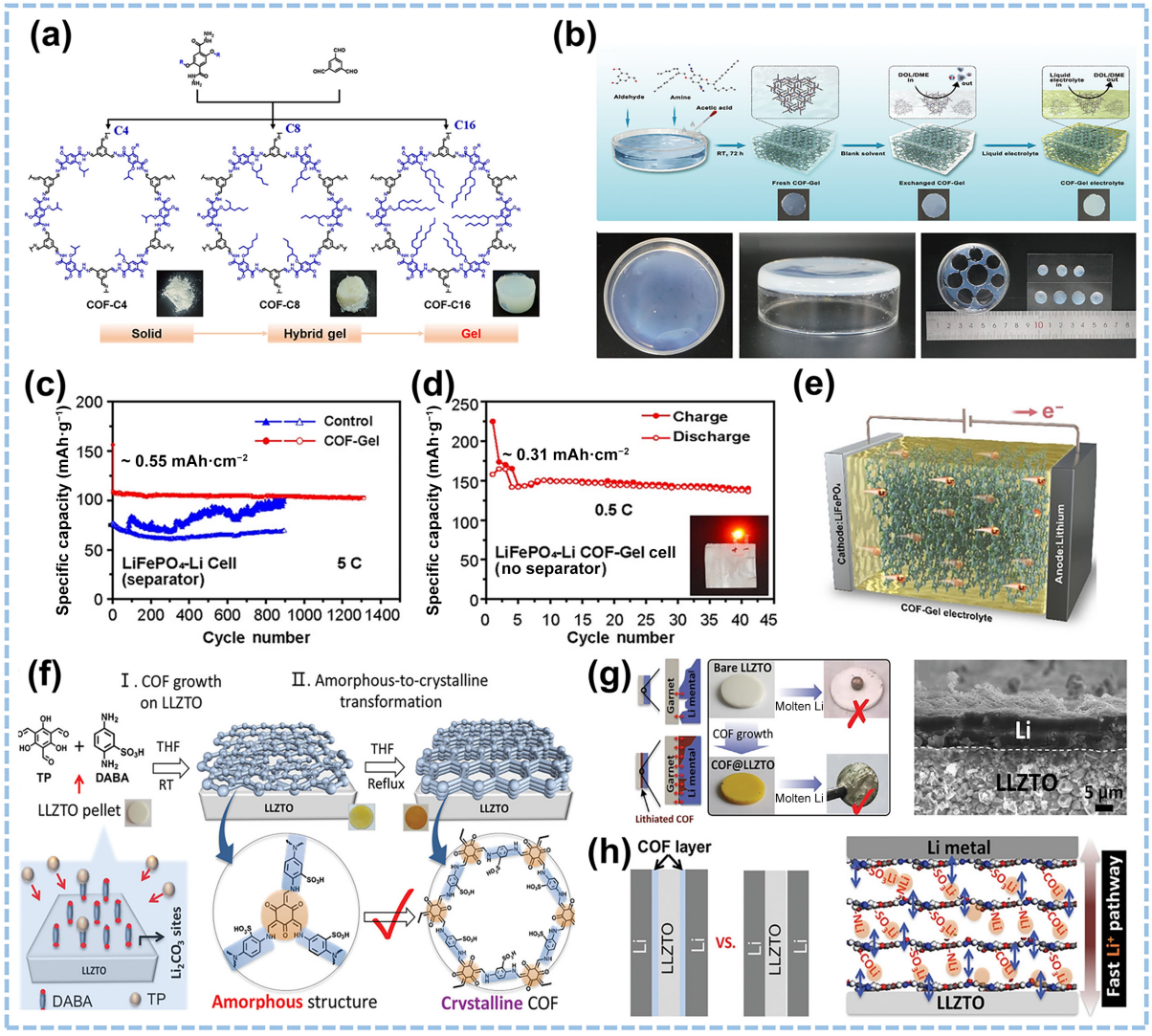

Figure 10 (a) Synthetic scheme of COF-C_x (x = 4, 8, and 16). (b) Detailed preparation process of the COF-Gel electrolyte. (c) Cycling performance of cells at 5 C after rate tests. (d) Cycling performance of cells at 0.5 C without separator skeleton. (e) Model of a CGE full battery. Reproduced with permission from Ref. [172], © Wiley-VCH GmbH 2021. (f) Synthetic scheme of c*sCOF@LLZTO SSE. (g) Comparison of infiltration properties of molten Li on LLZTO ceramics with/without sCOF layer and Cross-section scanning electron microscopy (SEM) image of the sCOF coated LLZTO pellet with Li metal. (h) Schematic of Li-Li symmetric cells with a*sCOF@LLZTO and c*sCOF@LLZTO SSEs, and the schematic of the possible Li^+ diffusion paths. Reproduced with permission from Ref. [173], © WILEY-VCH Verlag GmbH & Co. KGaA, Weinheim 2020.

interactions with the rigid framework and enhancing in-pore salt dissociation (Figs. 11(c) and 11(d)). The confined solvent environment produces a low-barrier and highly mobile conduction landscape, yielding an impressive room-temperature conductivity of 1.65×10^{-4} S·cm^{-1} and a transference number of 0.85. Notably, the resulting material forms ultrathin (~ 32 μm) and mechanically resilient films that preserve ionic conductivity even under repeated bending.

Paired with $LiFePO_4$ cathodes, DLC-based flexible solid-state cells demonstrate stable cycling under deformation, highlighting the promise of polymer-COF composite electrolytes for next-generation bendable and shape-conformal energy-storage technologies (Fig. 11(e)).

6 3D COF-based SSEs

Compared with conventional 2D COFs whose anisotropic pore channels restrict ion motion to in-plane directions, 3D COFs offer fully interconnected and multidirectional transport pathways. Their inherent topological complexity creates spacious and through-pore networks arising from tetrahedral nodes and 3D-crosslinked linkers, which differ fundamentally from the lamellar arrangements in 2D COFs. Although research on 3D COF-based SSEs remains in its infancy, pioneering studies have demonstrated their unique potential to combine structural rigidity, dynamic flexibility, and efficient ion transport within a single crystalline scaffold.

Most reported 3D COFs with tetrahedral connectivity are constructed from sp^3-hybridized carbon or silane nodes, which are often functionalized with flexible organic motifs such as cyclodextrins (CDs) [102, 123, 176, 177]. These linkers impart elasticity and internal dynamics essential for solid-state ion conduction, of which characteristics difficult to achieve in 2D COFs. The reversible covalent chemistry used during crystallization provides intrinsic error-correction, yielding well-defined lattices

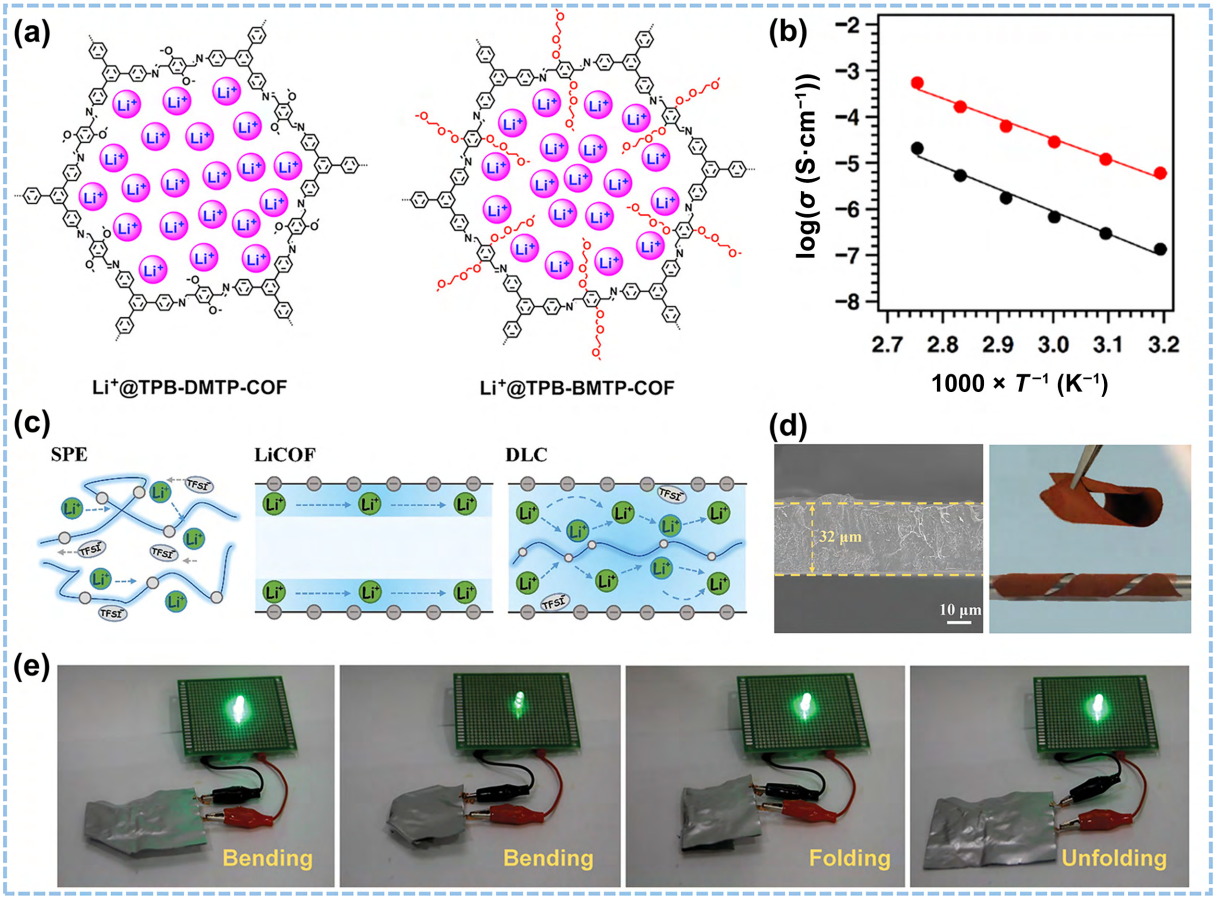

Figure 11 (a) Chemical structure of Li⁺@TPB-DMTP-COF and Li⁺@TPB-BMTP-COF with oligo(ethylene oxide). (b) Arrhenius plot of ionic conductivity of Li⁺@TPB-DMTP-COF (black) and Li⁺@TPB-BMTP-COF (red). Reproduced with permission from Ref. [147], © American Chemical Society 2018. (c) Illustration of the Li⁺ diffusion paths in conventional SPE, pristine LiCOF, and DLC. (d) Cross-sectional SEM image of the DLC electrolyte film. (e) Demonstration of a DLC-based pouch cell with digital photos of the bending and twisting of the DLC electrolyte. Reproduced with permission from Ref. [164], © Wiley-VCH GmbH 2022.

with minimized structural defects. When infiltrated with LEs, the resulting solvent-filled nanochannels offer densely populated functional sites capable of coordinating lithium salts, lowering ion dissociation barriers, and establishing continuous and low-energy ion-migration pathways. Owing to this combination of porosity, dynamic backbones, and ionic functionality, CD-based 3D COFs can simultaneously function as solid electrolytes and LE reservoirs, significantly enhancing ion-conduction kinetics [102].

6.1 Early demonstration of 3D CD-COFs in solid electrolytes

Zhang and co-workers reported the first demonstration of a 3D CD-COF serving as an SSE [123]. Crystalline 3D CD-COF powder was immersed in a 1.0 M $LiPF_6$ solution (ethylene carbonate (EC)/dimethyl carbonate (DMC) = 1:1 v/v) for 12 h, achieving a $LiPF_6$ uptake of 20 wt.%. After compaction, AC impedance spectroscopy revealed Arrhenius-type behavior with an activation energy of 0.26 eV (Fig. 12(a)). The ionic conductivity reached 0.27×10^{-3} S·cm^{-1} at 30 °C, comparable to gel polymer electrolytes, while maintaining long-range order and excellent thermal stability (Fig. 12(b)). The flexible and dynamic spiroborate linkages underpin the rapid Li$^+$ transport. The compatibility with lithium metal was confirmed using Li|3D CD-COF|Li symmetric cells operated at 0.085 mA·cm^{-2}, achieving stable cycling for 220 h with minimal polarization (Fig. 12(c)). The ionic backbone homogenizes ion flux and suppresses dendrite formation (Fig. 12(d)), establishing 3D CD-COFs as structurally robust and electrochemically stable SSE platforms.

3D COFs possess intrinsically interconnected and isotropic pore networks, providing continuous ion-transport pathways in all spatial directions, which is more favorable for homogeneous Li$^+$ flux regulation and mitigation of local current hotspots at the Li metal interface. Representative examples have demonstrated the promise of this structural evolution. For instance, crown ether-functionalized 3D COFs have been shown to enable uniform Li$^+$ coordination and transport throughout fully percolated pore networks, delivering high Li$^+$ transference numbers ($t_{Li^+} \approx 0.85$) and stable Li plating/stripping behavior [178]. Such isotropic transport pathways effectively suppress concentration polarization and dendrite nucleation, addressing limitations commonly observed in anisotropic 2D frameworks. In parallel, the development of self-catenated 3D COF topologies has markedly improved framework robustness and surface area, ensuring structural integrity under electrochemical operation while maintaining accessible ion-conduction channels [179].

Equally important is the growing ability to precisely engineer 3D COF architectures. Recent progress in stereoselective and topology-controlled synthesis has enabled fine regulation of pore size, connectivity, and local chemical environments in three dimensions, opening new opportunities to tailor Li$^+$ coordination chemistry and

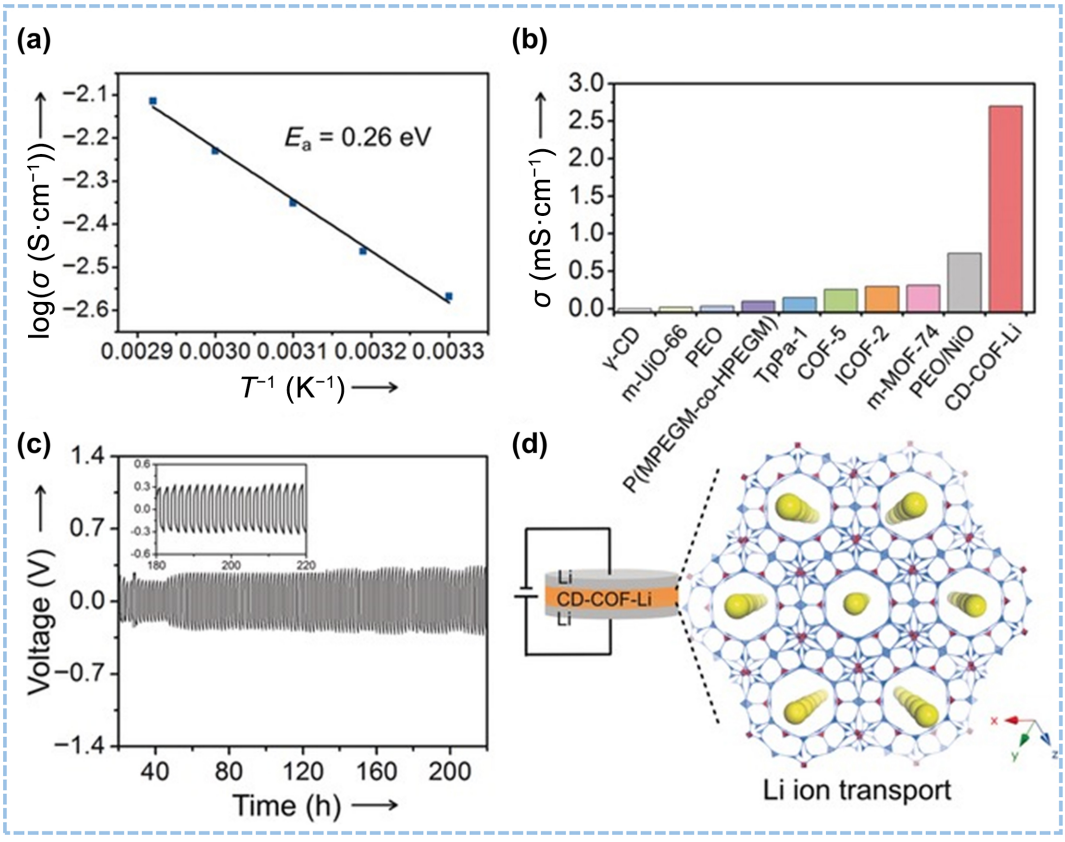

Figure 12 (a) Arrhenius plot of ionic conductivity with CD-COF Li-$LiPF_6$-EC-DMC. (b) Comparison of the ionic conductivity with literature-reported SSEs. (c) Li-Li symmetric cells with CD-COF Li-$LiPF_6$-EC-DMC at 0.085 mA·cm^{-2}. (d) The Li^+ diffusion paths of CD-COF-Li. Reproduced with permission from Ref. [123], © Wiley-VCH Verlag GmbH & Co. KGaA, Weinheim 2017.

transport kinetics [180]. Collectively, these advances indicate that 3D COFs are not merely structural analogues of their 2D counterparts, but represent a qualitatively distinct electrolyte design paradigm. By combining isotropic ion-conduction networks with enhanced mechanical and interfacial stability, 3D COF-based electrolytes provide a compelling pathway toward high-performance and durable solid-state lithium metal batteries.

6.2 Solvent-free 3D COFs for practical ASSLBs

Despite these advances, early systems relied on volatile carbonate solvents, limiting their safety and scalability. To overcome this barrier, Wang et al. incorporated a non-volatile plastic crystal (succinonitrile (SN)) into a spirobenzofuran-linked 3D COF (3D-SpCOF), yielding a solvent-free yet highly conductive SSE [177]. This design preserves the inherent porosity of the framework while eliminating flammable organic solvents.

Linear sweep voltammetry confirmed a wide electrochemical stability window up to 4.5 V (Fig. 13(a)). Impedance spectra of Li|3D-SpCOF-SSE|Li symmetric cells exhibited two distinct semicircles associated with bulk COF resistance and interfacial charge transfer, indicating the formation of a stable SEI at the COF/Li interface (Figs. 13(b) and 13(c)). Galvanostatic cycling revealed low interfacial resistance and excellent stability. The overpotential increased gradually with current density yet remained stable up to 0.3 mA·cm^{-2}, with polarization values of 50–235 mV across 0.05–0.25 mA·cm^{-2} (Figs. 13(d) and 13(e)). In full-cell tests, Li|3D-SpCOF-SSE|$LiFePO_4$ delivered steady cycling (Fig. 13(f)), while Li|3D-SpCOF-SSE|$LiCoO_2$ achieved 130, 120, and 75 mAh·g^{-1} at 54, 105, and 210 mA, respectively, sustaining high Coulombic efficiency over 300 cycles (Figs. 13(g) and 13(h)). These results highlight the practical viability of 3D COFs in ASSLBs.

6.3 3D anionic COFs for high-performance Li-O_2 batteries

Beyond traditional LIBs, 3D COF-based electrolytes have demonstrated compelling advantages for Li-O_2 batteries, where simultaneous requirements for safety, high ionic conductivity, chemical stability, and efficient gas transport converge. Wang and coworkers pioneered the synthesis of 3D anionic CD-COF-Li through a microwave-assisted solvothermal route, which is considered as an economical, scalable, and environmentally benign process [102]. By combining flexible CD nodes with complementary counterions, they generated a highly crystalline framework containing orderly aligned Li^+ channels.

Electrochemical impedance spectroscopy revealed an exceptionally high room-temperature ionic conductivity of 2.7 mS·cm^{-1}, surpassing most polymer or ceramic SSEs (Fig. 14(a)). The activation energy of 0.18 eV confirms the presence of continuous and low-barrier Li^+ pathways. Control experiments showed that the high conductivity originates from the intrinsic ionic channels rather than residual solvent. To exploit this framework in practical cathodes, CNTs were integrated with CD-COF-Li to construct a 3D and hierarchically conductive architecture (Fig. 14(b)). This design enables (i) electronic conduction through CNT networks, (ii) rapid Li^+ transport along COF nanochannels, and (iii) efficient O_2 diffusion through interparticle porosity which dramatically accelerating oxygen redox

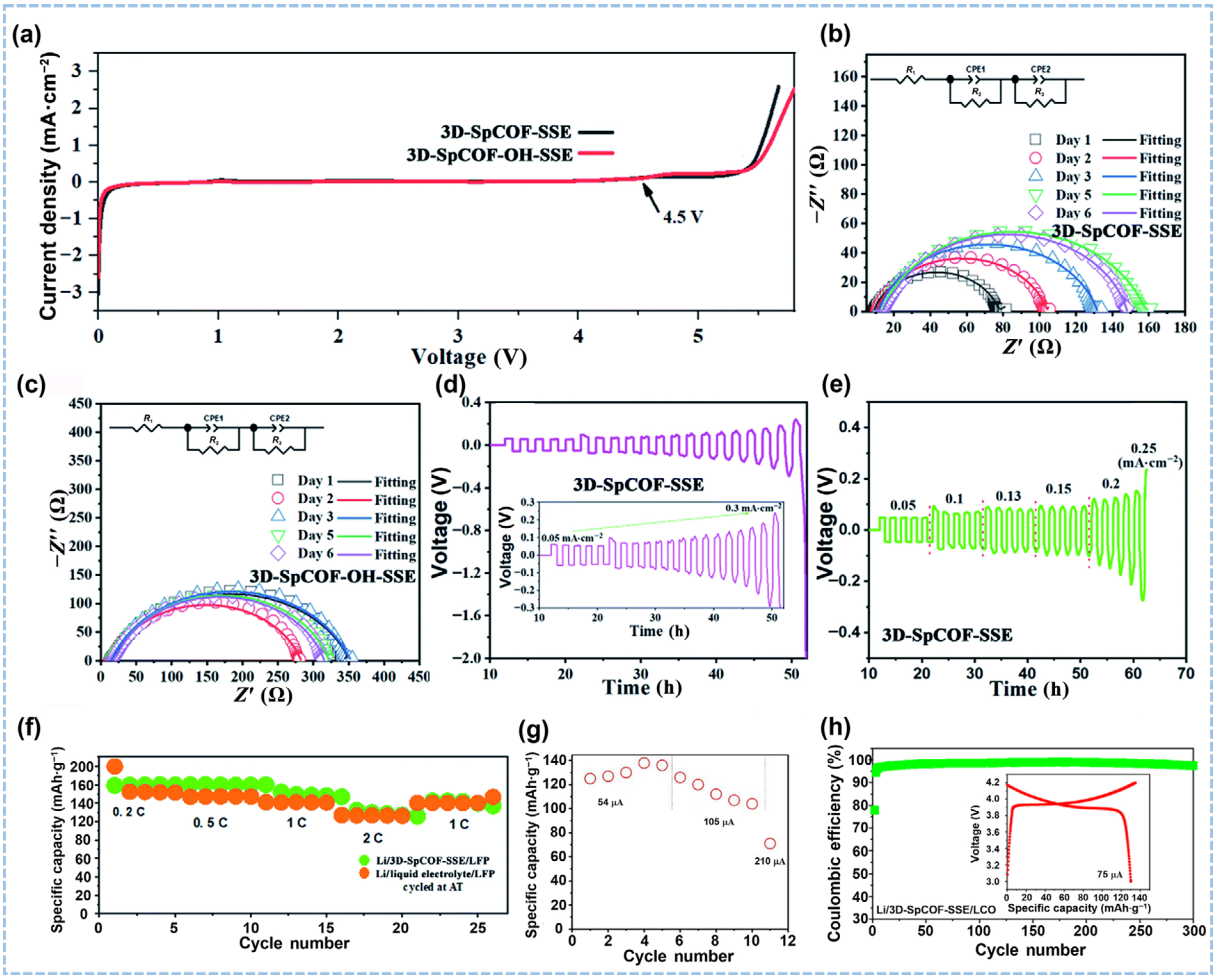

Figure 13 Electrochemical performance of SSEs. (a) LSVs and ((b) and (c)) electrochemical impedance spectroscopy (EIS) of Li-Li symmetric cells with 3D-SpCOF-SSE and 3D-SpCOF-OH-SSE. (d) Li-Li symmetric cells at step-increased current densities and (e) rate performance of the Li-Li cells. ((f) and (g)) Rate performance of the Li-LFP and Li-LCO batteries. (h) Coulombic efficiency of Li-LCO batteries for 300 cycles and the corresponding charge/discharge curves. Reproduced with permission from Ref. [177], © The Royal Society of Chemistry 2022.

kinetics. Solid-state Li-O_2 cells using CNT/CD-COF-Li delivered first-cycle discharge and charge capacities of 9340 and 8200 mAh·g^{-1}, respectively, outperforming CNT/PEO and CNT/LAGP counterparts (Fig. 14(c)). At a fixed capacity of 500 mAh·g^{-1} and 200 mA·g^{-1}, the CNT/CD-COF-Li cell sustained 100 cycles, whereas CNT/PEO and CNT/LAGP cells failed after 38 and 50 cycles, respectively (Fig. 14(d)). These results establish 3D anionic COFs as a high-performance SSE class capable of meeting the stringent requirements of next-generation Li-O_2 systems.

7 Summaries and perspectives

COF-based 2D/3D SSEs have emerged as a structurally tunable platform capable of addressing several long-standing bottlenecks associated with conventional ceramic and polymer electrolytes. By thoughtfully modifying and selecting organic linkers, as well as utilizing post-synthesis modifications of COFs, functional 2D/3D COFs can be constructed with a range of desirable properties, such as excellent chemical and thermal stability, adjustable pore sizes, outstanding ion conductivity, and superior flexibility. From a practical perspective, the large-scale deployment of COF-based SSEs will critically depend on advancements in sustainable synthesis and manufacturability. Emerging strategies, including the use of biomass-derived monomers, green reaction media (e.g., water, ionic liquids, or deep eutectic solvents), and solvent-free mechanochemical routes, offer promising pathways to reduce cost and environmental footprint. In parallel, transitioning from batch solvothermal synthesis to energy-efficient and scalable techniques, such as microwave-assisted or continuous processing, will be essential. All these aspects render COFs for competitive conductivity, superior interfacial stability, and improved safety, thereby challenging the long-held dominance of conventional SSE systems. Their construction from lightweight elements further enhances the gravimetric energy density of ASSLBs, a point emphasized earlier in the discussions of materials selection and structural optimization.

Despite their promise, COF-SSEs still face the persistent challenges that permeate the broader field of solid-state lithium-metal batteries: high reactivity toward Li metal and non-uniform Li deposition. As discussed above, solvent residues often unavoidable during COF synthesis or pore activation can aggravate these issues by narrowing the electrochemical stability window and weakening interfacial integrity. It was revealed that residual solvents play a dual role: (i) dissolving/dissociating lithium salts to accelerate Li^+ migration, and (ii) plasticizing the framework to alleviate mechanical brittleness. However, the subsequent emergence of

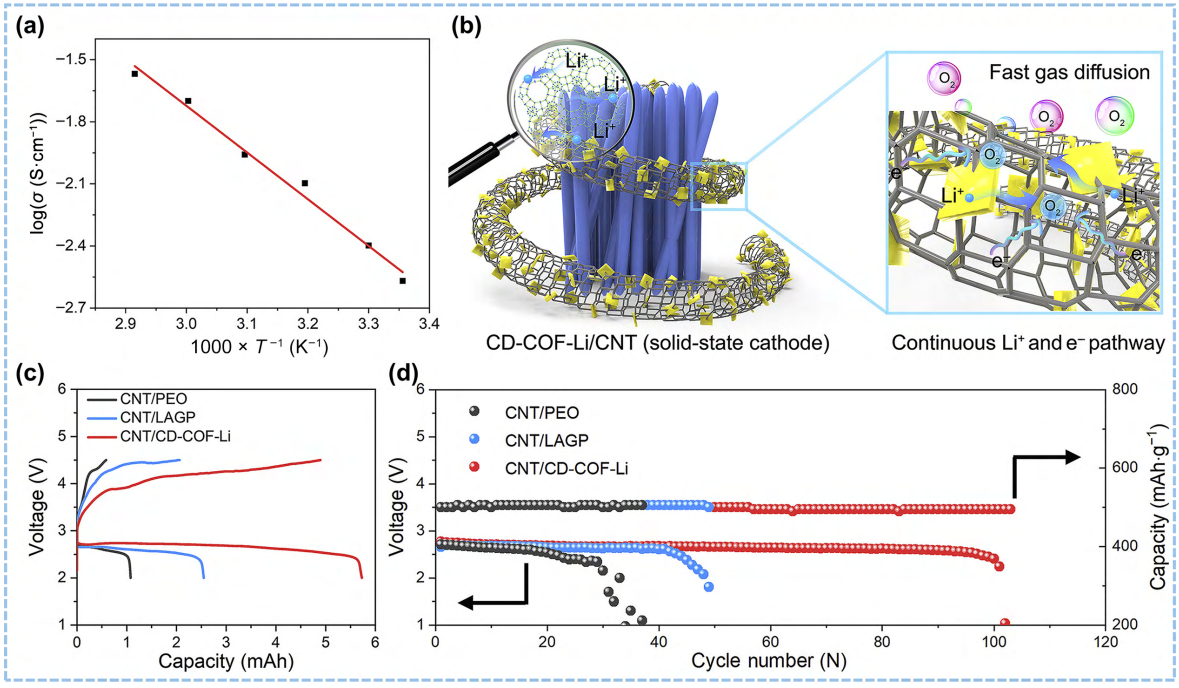

Figure 14 (a) Arrhenius plot of ionic conductivity of CD-COF-Li at various temperatures. (b) Schematic diagram of the CD-COF-Li/CNT. Electrochemical performance of solid-state Li-O_2 batteries of (c) charge/discharge voltage profiles and (d) cycling performance. Reproduced with permission from Ref. [102], © Elsevier Inc. 2022.

solvent-free COF-SSEs with lower impedance and superior cycling demonstrates that intrinsically fast Li^+ transport can be achieved solely through precise manipulation of the framework topology, linkage chemistry, and pore environment, an observation that aligns with earlier discussions of backbone polarity and channel geometry.

Looking forward, the continued evolution of COF-SSEs will depend on a coordinated effort along several research directions:

(i) Backbone and pore-environment engineering

Building on insights from Sections 2–4, future COFs should leverage polar/ionic functional groups (e.g., sulfonates, acetates, and imidazolium units) to regulate site-specific ion coordination, immobilize anions, and approach unity Li^+ transference number. Coulombic repulsion or tailored electrostatic fields within confined channels may simultaneously suppress anion drift and lower activation barriers for Li^+ hopping, moving toward truly decoupled ion conduction.

(ii) Quasi-solid and hybrid COF architectures

Consistent with discussions in Section 5, integrating non-volatile ionic liquids, polymer gels, or solid plasticizers into COF nanochannels may combine the structural order of COFs with the adaptability of soft phases. Such quasi-solid systems could widen the electrochemical window, enhance mechanical compliance, and deliver more intimate and defect-free interfaces with Li metal.

(iii) Advanced mechanistic understanding

To complete the structure–property correlation framework outlined earlier, fundamental studies should quantify the density and binding strength of active sites, clarify the Li^+ coordination environment, and link crystal orientation or domain size with through-plane conductivity. Understanding how Li salts interact with backbone conformation and dynamic pore breathing will be essential for predictive design and performance optimization.

(iv) Dendrite suppression via channel-guided flux

Echoing the interfacial instability issues highlighted in Section 6, the uniform angstrom-to-nanometer-scaled channels of COFs provide a distinctive opportunity to modulate Li^+ flux, homogenize current distribution, and promote planar Li deposition. Establishing universal metrics (e.g., critical current density and single-cycle stripping/plating stability) and their correlation with interfacial chemistry will be central to enabling safe Li metal cycling.

Nevertheless, the path toward commercialization will ultimately depend on resolving two overarching barriers that were implicit throughout the earlier sections:

(1) Processability and scalable fabrication

Most existing COF-SSEs rely on cold-pressed pellets that are rigid, thick, and incompatible with practical cell assembly. Beyond intrinsic brittleness, the poor solid–solid contact between pelletized COFs and electrodes often leads to high interfacial resistance, further limiting practical performance.

Techniques such as solution-processable COF dispersions, thin-film coating, interfacial polymerization, or direct-growth methods must be developed to yield flexible, defect-minimized, and Li-wettable membranes. In particular, *in-situ* growth or polymerization of COF layers directly on electrode surfaces offers a promising route to achieve conformal and low-impedance interfaces at the molecular level.

From a manufacturing perspective, mixed-matrix membranes (MMMs), in which COFs are embedded as functional fillers within flexible polymer matrices, and ultrathin supported COF membranes are fabricated on commercial porous separators via interfacial growth or coating, and provide practical pathways toward large-area and roll-to-roll-compatible production. Achieving industrially scalable architectures is arguably as important as improving intrinsic conductivity.

(2) Intrinsic ionic conductivity

Although COF-SSEs have demonstrated conductivities exceeding 10^{-3} S·cm^{-1}, further improvements such as approaching or surpassing state-of-the-art inorganic/PEO composite benchmarks remain crucial for high-rate operation. These advances will rely on

deeper mechanistic insight into Li^+–pore interactions, rational tuning of channel polarity, and optimization of long-range structural coherence. In parallel, interfacial engineering strategies, including the introduction of ultrathin soft buffering layers (e.g., polymer interlayers, ionic liquids, or plastic-crystal phases), may synergistically reduce interfacial impedance while preserving fast ion transport.

By systematically addressing these challenges while building upon the structure–transport–interface paradigm established throughout this review, COF-based SSEs are poised to evolve from laboratory exploration to commercially enabling technologies. With their intrinsic modularity, chemical diversity, and compatibility with next-generation Li metal anodes, COF-SSEs hold strong potential to define the next wave of safe, high-energy, and durable solid-state battery systems.

Data availability

Not applicable.

Acknowledgements

The authors acknowledge funding support from the National Natural Science Foundation of China (Nos. 22309003 and 52402299), the Fundamental Research Funds for the Central Universities (No. 2682025CX011), the Science Fund for Excellent Young Scholars of Anhui Province (No. 2508085Y010), and the Natural Science Research Project of Anhui Province Education Department (No. 2023AH051119). The authors also thank the support from the Scientific Compass (www.shiyanjia.com).

Declaration of competing interest

All the contributing authors report no conflict of interests in this work.

Author contribution statement

Q. Y. D.: Literatures collection, formal analysis, writing – original draft. Y. W.: Formal analysis, writing – original draft preparation. Z. Y. Z.: Formal analysis, writing – original draft preparation. Y. J. C.: Formal analysis, writing – original draft preparation. C. D. W.: Formal analysis, writing – original draft preparation. D. L. X.: Supervision, data curation, writing – review & editing. Q. K.: Supervision, data curation, writing – review & editing, funding acquisition. L. B. M.: Supervision, data curation, writing – review & editing, funding acquisition. J. X.: Supervision, data curation, writing – review & editing, funding acquisition. All the authors have approved the final manuscript.

Use of AI statement

None.

References

[1] Fierer, N. Earthworms' place on Earth. *Science* **2019**, *366*, 425–426.
[2] Huang, Z. Y.; Deng, Z.; Zhong, Y.; Xu, M. K.; Li, S. D.; Liu, X. T.; Zhou, Y.; Huang, K.; Shen, Y.; Huang, Y. H. Progress and challenges of prelithiation technology for lithium-ion battery. *Carbon Energy* **2022**, *4*, 1107–1132.
[3] Chow, J.; Kopp, R. J.; Portney, P. R. Energy resources and global development. *Science* **2003**, *302*, 1528–1531.
[4] Kang, B.; Ceder, G. Battery materials for ultrafast charging and discharging. *Nature* **2009**, *458*, 190–193.
[5] He, Q. J.; Deng, Z. W.; Miao, S. C.; Jia, Y.; Peng, J. N.; Xia, P. F.; Xu, C. H. Y.; Tang, Q.; Zhang, X. M.; Tan, T. N. et al. An anion outer-regulated electrolyte allows rapid desolvation to enable high-voltage lithium metal batteries. *Energy Environ. Sci.* **2025**, *18*, 9093–9104.
[6] Tang, G. B.; Li, Y.; Wu, J. X.; Kang, Q.; Ma, L. B. Engineering heterostructured electrocatalysts for enhanced sulfur redox kinetics in metal-sulfur batteries. *Nano Res. Energy* **2025**, *4*, e9120179.
[7] McSweeney, W.; Geaney, H.; O'Dwyer, C. Metal-assisted chemical etching of silicon and the behavior of nanoscale silicon materials as Li-ion battery anodes. *Nano Res.* **2015**, *8*, 1395–1442.
[8] Deng, Z. W.; Jia, Y.; Deng, Y.; Xu, C. H. Y.; Zhang, X. M.; He, Q. J.; Peng, J. N.; Wu, H.; Cai, W. L. Coordination structure regulation in non-flammable electrolyte enabling high voltage lithium electrochemistry. *J. Energy Chem.* **2024**, *96*, 282–290.
[9] Balke, N.; Jesse, S.; Morozovska, A. N.;Eliseev, E.;Chung, D. W.;Kim, Y.;Adamczyk, L.;García, R. E.;Dudney, N.; Kalinin, S. V. Nanoscale mapping of ion diffusion in a lithium-ion battery cathode. *Nat. Nanotechnol.* **2010**, *5*, 749–754.
[10] Chen, M. Y.; Ma, X. T.; Chen, B.; Arsenault, R.; Karlson, P.; Simon, N.; Wang, Y. Recycling end-of-life electric vehicle lithium-ion batteries. *Joule* **2019**, *3*, 2622–2646.
[11] Griffith, K. J.; Wiaderek, K. M.; Cibin, G.; Marbella, L. E.; Grey, C. P. Niobium tungsten oxides for high-rate lithium-ion energy storage. *Nature* **2018**, *559*, 556–563.
[12] Harper, G.; Sommerville, R.; Kendrick, E.; Driscoll, L.; Slater, P.; Stolkin, R.; Walton, A.; Christensen, P.; Heidrich, O.; Lambert, S. et al. Recycling lithium-ion batteries from electric vehicles. *Nature* **2019**, *575*, 75–86.
[13] Johnson, C. S. Charging up lithium-ion battery cathodes. *Joule* **2018**, *2*, 373–375.
[14] Chu, L. H.; Shi, Y. X.; Li, Z.; Sun, C. X.; Yan, H.; Ma, J.; Li, X. C.; Liu, C. F.; Gu, J. N.; Liu, K. et al. Solid electrolyte interphase on anodes in rechargeable lithium batteries. *Nano Res.* **2023**, *16*, 11589–11603.
[15] Liu, X.; Ren, D. S.; Hsu, H.; Feng, X. N.; Xu, G. L.; Zhuang, M. H.; Gao, H.; Lu, L. G.; Han, X. B.; Chu, Z. Y. et al. Thermal runaway of lithium-ion batteries without internal short circuit. *Joule* **2018**, *2*, 2047–2064.
[16] Lu, J.; Wu, T. P.; Amine, K. State-of-the-art characterization techniques for advanced lithium-ion batteries. *Nat. Energy* **2017**, *2*, 17011.
[17] Sasaki, T.; Ukyo, Y.; Novák, P. Memory effect in a lithium-ion battery. *Nat. Mater.* **2013**, *12*, 569–575.
[18] Lagadec, M. F.; Zahn, R.; Wood, V. Characterization and performance evaluation of lithium-ion battery separators. *Nat. Energy* **2019**, *4*, 16–25.
[19] Lin, X. K.; Khosravinia, K.; Hu, X. S.; Li, J.; Lu, W. Lithium plating mechanism, detection, and mitigation in lithium-ion batteries. *Prog. Energy Combust. Sci.* **2021**, *87*, 100953.
[20] Ma, X. T.; Chen, M. Y.; Zheng, Z. F.; Bullen, D.; Wang, J.; Harrison, C.; Gratz, E.; Lin, Y. L.; Yang, Z. Z.; Zhang, Y. T. et al. Recycled cathode materials enabled superior performance for lithium-ion batteries. *Joule* **2021**, *5*, 2955–2970.
[21] Nolan, A. M.; Zhu, Y. Z.; He, X. F.; Bai, Q.; Mo, Y. F. Computation-accelerated design of materials and interfaces for all-solid-state lithium-ion batteries. *Joule* **2018**, *2*, 2016–2046.
[22] Wang, C. Y.; Zhang, G. S.; Ge, S. H.; Xu, T.; Ji, Y.; Yang, X. G.; Leng, Y. J. Lithium-ion battery structure that self-heats at low temperatures. *Nature* **2016**, *529*, 515–518.
[23] Yang, C. Y.; Chen, J.; Ji, X.; Pollard, T. P.; Lü, X. J.; Sun, C. J.; Hou, S.; Liu, Q.; Liu, C. M.; Qing, T. T. et al. Aqueous Li-ion battery enabled by halogen conversion-intercalation chemistry in graphite. *Nature* **2019**, *569*, 245–250.

[24] Heiskanen, S. K.; Kim, J.; Lucht, B. L. Generation and evolution of the solid electrolyte interphase of lithium-ion batteries. *Joule* **2019**, *3*, 2322–2333.

[25] Xu, C. H. Y.; Jing, P.; Xia, P. F.; Jia, Y.; Peng, J. N.; He, Q. J.; Liu, Q. Q.; Song, Z. M.; Zhang, X. M.; Wu, F. L. et al. Tailoring a multilayer fine-grained solid electrolyte interphase by pulse electrochemical activation maneuver for stable Si/C anodes. *Energy Environ. Sci.* **2025**, *18*, 7060–7070.

[26] Piao, Z. H.; Xiao, P. T.; Luo, R. P.; Ma, J. B.; Gao, R. H.; Li, C.; Tan, J. Y.; Yu, K.; Zhou, G. M.; Cheng, H. M. Constructing a stable interface layer by tailoring solvation chemistry in carbonate electrolytes for high-performance lithium-metal batteries. *Adv. Mater.* **2022**, *34*, 2108400.

[27] Yang, Y. X.; Zhang, C. H.; Mei, Z. Y.; Sun, Y. J.; An, Q.; Jing, Q.; Zhao, G. F.; Guo, H. Interfacial engineering of perfluoroalkyl functionalized covalent organic framework achieved ultra-long cycled and dendrite-free lithium anodes. *Nano Res.* **2023**, *16*, 9289–9298.

[28] Adenusi, H.; Chass, G. A.; Passerini, S.; Tian, K. V.; Chen, G. H. Lithium batteries and the solid electrolyte interphase (SEI)-progress and outlook. *Adv. Energy Mater.* **2023**, *13*, 2203307.

[29] Hatzell, K. B.; Chen, X. C.; Cobb, C. L.; Dasgupta, N. P.; Dixit, M. B.; Marbella, L. E.; McDowell, M. T.; Mukherjee, P. P.; Verma, A.; Viswanathan, V. et al. Challenges in lithium metal anodes for solid-state batteries. *ACS Energy Lett.* **2020**, *5*, 922–934.

[30] Li, Y.; Liu, M. Q.; Feng, X.; Li, Y.; Wu, F.; Bai, Y.; Wu, C. How can the electrode influence the formation of the solid electrolyte interface. *ACS Energy Lett.* **2021**, *6*, 3307–3320.

[31] Zhao, L. H.; Sottos, N. R. Autonomous strategies for improved performance and reliability of Li-ion batteries. *Adv. Energy Mater.* **2021**, *11*, 2003139.

[32] Chae, O. B.; Lucht, B. L. Interfacial issues and modification of solid electrolyte interphase for Li metal anode in liquid and solid electrolytes. *Adv. Energy Mater.* **2023**, *13*, 2203791.

[33] Shi, Q. T.; Zhou, J. H.; Ullah, S.; Yang, X. Q.; Tokarska, K.; Trzebicka, B.; Ta, H. Q.; Rümmeli, M. H. A review of recent developments in Si/C composite materials for Li-ion batteries. *Energy Storage Mater.* **2021**, *34*, 735–754.

[34] Zhang, S. L.; Ying, H. J.; Yuan, B.; Hu, R. Z.; Han, W. Q. Partial atomic tin nanocomplex pillared few-layered $Ti_3C_2T_x$ MXenes for superior lithium-ion storage. *Nano-Micro Lett.* **2020**, *12*, 78.

[35] Wang, J. Y.; Huang, W.; Pei, A.; Li, Y. Z.; Shi, F. F.; Yu, X. Y.; Cui, Y. Improving cyclability of Li metal batteries at elevated temperatures and its origin revealed by cryo-electron microscopy. *Nat. Energy* **2019**, *4*, 664–670.

[36] Tavassol, H.; Jones, E. M. C.; Sottos, N. R.; Gewirth, A. A. Electrochemical stiffness in lithium-ion batteries. *Nat. Mater.* **2016**, *15*, 1182–1187.

[37] Peng, L. S.; Wu, X. K.; Jia, M. M.; Qian, W. W.; Zhang, X. Y.; Zhou, N.; Zhang, L.; Jian, C. Y.; Zhang, S. J. Solvating power regulation enabled low concentration electrolyte for lithium batteries. *Sci. Bull.* **2022**, *67*, 2235–2244.

[38] Gao, Z. H.; Sun, H. B.; Fu, L.; Ye, F. L.; Zhang, Y.; Luo, W.; Huang, Y. H. Promises, challenges, and recent progress of inorganic solid-state electrolytes for all-solid-state lithium batteries. *Adv. Mater.* **2018**, *30*, 1705702.

[39] Jo, C. H.; Sohn, K. S.; Myung, S. T. Feasible approaches for anode-free lithium-metal batteries as next generation energy storage systems. *Energy Storage Mater.* **2023**, *57*, 471–496.

[40] Zheng, Z. Y.; Zhang, W. C.; Dai, Q. Y.; Wu, H. S.; Huang, Z. W.; Zhang, Y. N.; Peng, B.; Ma, L. B.; Xu, J. Regulating the anionic environment of the COF@CNT composite for kinetics-boosted and wide-temperature lithium-sulfur batteries. *J. Mater. Chem. A* **2025**, *13*, 26288–26296.

[41] Xu, C. H. Y.; Jing, P.; Deng, Z. W.; Liu, Q. Q.; Jia, Y.; Zhang, X. M.; Deng, Y.; Zhang, Y.; Cai, W. L. Rectifying solid electrolyte interphase structure for stable multi-dimensional silicon anodes. *Energy Storage Mater.* **2025**, *74*, 103911.

[42] Zhang, Y.; Zhang, L.; Guo, P.; Zhang, C. Y.; Ren, X. C.; Jiang, Z.; Song, J. J.; Shi, C. Porous garnet as filler of solid polymer electrolytes to enhance the performance of solid-state lithium batteries. *Nano Res.* **2024**, *17*, 2663–2670.

[43] Janek, J.; Zeier, W. G. Challenges in speeding up solid-state battery development. *Nat. Energy* **2023**, *8*, 230–240.

[44] Shao, B. W.; Huang, Y. L.; Han, F. D. Electronic conductivity of lithium solid electrolytes. *Adv. Energy Mater.* **2023**, *13*, 2204098.

[45] Xia, S. X.; Wu, X. S.; Zhang, Z. C.; Cui, Y.; Liu, W. Practical challenges and future perspectives of all-solid-state lithium-metal batteries. *Chem* **2019**, *5*, 753–785.

[46] Bachman, J. C.; Muy, S.; Grimaud, A.; Chang, H. H.; Pour, N.; Lux, S. F.; Paschos, O.; Maglia, F.; Lupart, S.; Lamp, P. et al. Inorganic solid-state electrolytes for lithium batteries: Mechanisms and properties governing ion conduction. *Chem. Rev.* **2016**, *116*, 140–162.

[47] Zhang, H.; Li, C. M.; Piszcz, M.; Coya, E.; Rojo, T.; Rodriguez-Martinez, L. M.; Armand, M.; Zhou, Z. B. Single lithium-ion conducting solid polymer electrolytes: Advances and perspectives. *Chem. Soc. Rev.* **2017**, *46*, 797–815.

[48] Lau, J.; DeBlock, R. H.; Butts, D. M.; Ashby, D. S.; Choi, C. S.; Dunn, B. S. Sulfide solid electrolytes for lithium battery applications. *Adv. Energy Mater.* **2018**, *8*, 1800933.

[49] Fan, L.; Wei, S. Y.; Li, S. Y.; Li, Q.; Lu, Y. Y. Recent progress of the solid-state electrolytes for high-energy metal-based batteries. *Adv. Energy Mater.* **2018**, *8*, 1702657.

[50] McConohy, G.; Xu, X.; Cui, T.; Barks, E.; Wang, S.; Kaeli, E.; Melamed, C.; Gu, X. W.; Chueh, W. C. Mechanical regulation of lithium intrusion probability in garnet solid electrolytes. *Nat. Energy* **2023**, *8*, 241–250.

[51] Liu, M.; Zhang, S. N.; Van Eck, E. R. H.; Wang, C.; Ganapathy, S.; Wagemaker, M. Improving Li-ion interfacial transport in hybrid solid electrolytes. *Nat. Nanotechnol.* **2022**, *17*, 959–967.

[52] Fan, X. Y.; Zhong, C.; Liu, J.; Ding, J.; Deng, Y. D.; Han, X. P.; Zhang, L.; Hu, W. B.; Wilkinson, D. P.; Zhang, J. J. Opportunities of flexible and portable electrochemical devices for energy storage: Expanding the spotlight onto semi-solid/solid electrolytes. *Chem. Rev.* **2022**, *122*, 17155–17239.

[53] Huo, S. D.; Sheng, L.; Xue, W. D.; Wang, L.; Xu, H.; Zhang, H.; He, X. M. Challenges of polymer electrolyte with wide electrochemical window for high energy solid-state lithium batteries. *InfoMat* **2023**, *5*, e12394.

[54] Famprikis, T.; Canepa, P.; Dawson, J. A.; Islam, M. S.; Masquelier, C. Fundamentals of inorganic solid-state electrolytes for batteries. *Nat. Mater.* **2019**, *18*, 1278–1291.

[55] Cheng, X. B.; Zhao, C. Z.; Yao, Y. X.; Liu, H.; Zhang, Q. Recent advances in energy chemistry between solid-state electrolyte and safe lithium-metal anodes. *Chem* **2019**, *5*, 74–96.

[56] Fan, Z. J.; Ding, B.; Li, Z. W.; Hu, B.; Xu, C.; Xu, C. Y.; Dou, H.; Zhang, X. G. Long-cycling all-solid-state batteries achieved by 2D interface between prelithiated aluminum foil anode and sulfide electrolyte. *Small* **2022**, *18*, 2204037.

[57] Ding, B.; Wang, J.; Fan, Z. J.; Chen, S.; Lin, Q. Y.; Lu, X. J.; Dou, H.; Kumar Nanjundan, A.; Yushin, G.; Zhang, X. G. et al. Solid-state lithium-sulfur batteries: Advances, challenges and perspectives. *Mater. Today* **2020**, *40*, 114–131.

[58] Zhang, B. K.; Tan, R.; Yang, L. Y.; Zheng, J. X.; Zhang, K. C.; Mo, S. J.; Lin, Z.; Pan, F. Mechanisms and properties of ion-transport in inorganic solid electrolytes. *Energy Storage Mater.* **2018**, *10*, 139–159.

[59] Wang, X. E.; Zhang, C.; Sawczyk, M.; Sun, J.; Yuan, Q. H.; Chen, F. F.; Mendes, T. C.; Howlett, P. C.; Fu, C. K.; Wang, Y. Q. et al. Ultra-stable all-solid-state sodium metal batteries enabled by perfluoropolyether-based electrolytes. *Nat. Mater.* **2022**, *21*, 1057–1065.

[60] Liang, Q.; Chen, L. N.; Tang, J. Y.; Liu, X. Z.; Liu, J. J.; Tang, M.; Wang, Z. B. Large-scale preparation of ultrathin composite polymer electrolytes with excellent mechanical properties and high thermal stability for solid-state lithium-metal batteries. *Energy Storage Mater.* **2023**, *55*, 847–856.

[61] Zhang, X. Y.; Fu, C. K.; Cheng, S. C.; Zhang, C. B.; Zhang, L. C.; Jiang, M.; Wang, J. J.; Ma, Y. L.; Zuo, P. J.; Du, C. Y. et al. Novel PEO-based composite electrolyte for low-temperature all-solid-state lithium metal batteries enabled by interfacial cation-assistance. *Energy Storage Mater.* **2023**, *56*, 121–131.

[62] Wu, J. Y.; Rao, Z. X.; Cheng, Z. X.; Yuan, L. X.; Li, Z.; Huang, Y. H. Ultrathin, flexible polymer electrolyte for cost-effective fabrication of all-solid-state lithium metal batteries. *Adv. Energy Mater.* **2019**, *9*, 1902767.

[63] Choo, Y.; Halat, D. M.; Villaluenga, I.; Timachova, K.; Balsara, N. P. Diffusion and migration in polymer electrolytes. *Prog. Polym. Sci.* **2020**, *103*, 101220.

[64] Tilford, R. W.; Gemmill, W. R.; Zur Loye, H. C.; Lavigne, J. J. Facile synthesis of a highly crystalline, covalently linked porous boronate network. *Chem. Mater.* **2006**, *18*, 5296–5301.

[65] Côté, A. P.; Benin, A. I.; Ockwig, N. W.; O'Keeffe, M.; Matzger, A. J.; Yaghi, O. M. Porous, crystalline, covalent organic frameworks. *Science* **2005**, *310*, 1166–1170.

[66] Zhou, Z. B.; Han, X. H.; Qi, Q. Y.; Gan, S. X.; Ma, D. L.; Zhao, X. A facile, efficient, and general synthetic method to amide-linked covalent organic frameworks. *J. Am. Chem. Soc.* **2022**, *144*, 1138–1143.

[67] Liu, J.; Zhang, J. P.; Zhu, J.; Zhao, R. Q.; Zhang, Y. M.; Ma, Y. F.; Li, C. X.; Zhang, H. T.; Chen, Y. S. A lithium sulfonylimide COF-modified separator for high-performance Li-S batteries. *Nano Res.* **2023**, *16*, 12601–12607.

[68] Dey, K.; Pal, M.; Rout, K. C.; Kunjattu H, S.; Das, A.; Mukherjee, R.; Kharul, U. K.; Banerjee, R. Selective molecular separation by interfacially crystallized covalent organic framework thin films. *J. Am. Chem. Soc.* **2017**, *139*, 13083–13091.

[69] Geng, K. Y.; Arumugam, V.; Xu, H. J.; Gao, Y. N.; Jiang, D. L. Covalent organic frameworks: Polymer chemistry and functional design. *Prog. Polym. Sci.* **2020**, *108*, 101288.

[70] Song, R. Z.; Tan, B. E.; Gao, H. Progress in covalent organic frameworks based electrolytes: Synthesis, design and application in lithium metal batteries. *Coord. Chem. Rev.* **2026**, *553*, 217539.

[71] Zhu, L. Y.; Cao, Y.; Xu, T.; Yang, H. B.; Wang, L. Y.; Dai, L.; Pan, F. S.; Chen, C. J.; Si, C. L. Covalent organic framework membranes for energy storage and conversion. *Energy Environ. Sci.* **2025**, *18*, 5675–5739.

[72] Geng, K. Y.; He, T.; Liu, R. Y.; Dalapati, S.; Tan, K. T.; Li, Z. P.; Tao, S. S.; Gong, Y. F.; Jiang, Q. H.; Jiang, D. L. Covalent organic frameworks: Design, synthesis, and functions. *Chem. Rev.* **2020**, *120*, 8814–8933.

[73] Xu, J.; Dai, Q. Y.; Yang, Y. T.; Zheng, Z. Y.; Yu, F. T.; Cao, Y. J.; Jiang, Z. P.; Peng, B.; Ma, L. B. Wide-temperature zinc-iodine batteries enabling by a Zn-ion conducting covalent organic framework buffer layer. *Chem. Eng. J.* **2024**, *502*, 157984.

[74] Huang, N.; Wang, P.; Jiang, D. L. Covalent organic frameworks: a materials platform for structural and functional designs. *Nat. Rev. Mater.* **2016**, *1*, 16068.

[75] Wang, P. L.; Ding, S. Y.; Zhang, Z. C.; Wang, Z. P.; Wang, W. Constructing robust covalent organic frameworks via multicomponent reactions. *J. Am. Chem. Soc.* **2019**, *141*, 18004–18008.

[76] Lyle, S. J.; Waller, P. J.; Yaghi, O. M. Covalent organic frameworks: Organic chemistry extended into two and three dimensions. *Trends Chem.* **2019**, *1*, 172–184.

[77] Kandambeth, S.; Dey, K.; Banerjee, R. Covalent organic frameworks: Chemistry beyond the structure. *J. Am. Chem. Soc.* **2019**, *141*, 1807–1822.

[78] Gu, M. H.; Wu, J. X.; Li, C.; Zhang, Z. Y.; Wu, Y. R.; Cheng, X. L.; Li, R. J.; Tian, Y.; Bang, K. T.; Wang, R. et al. Mechanically assisted Li^+-conduction in crown ether-covalent organic frameworks for lithium metal batteries. *Adv. Mater.* **2026**, *38*, e11473.

[79] Hu, B.; Xu, J.; Fan, Z. J.; Xu, C.; Han, S. C.; Zhang, J. X.; Ma, L. B.; Ding, B.; Zhuang, Z. C.; Kang, Q. et al. Covalent organic framework based lithium-sulfur batteries: Materials, interfaces, and solid-state electrolytes. *Adv. Energy Mater.* **2023**, *13*, 2203540.

[80] Zha, X. L.; Zuo, M. J.; Xu, G. L.; Yan, Z.; You, H. N.; Xiong, Y.; Liu, Y.; Li, Y. Y.; Yang, L. Y.; Liu, K. et al. Chiral transfer amidst one-dimensional linear polymers and two-dimensional network covalent organic frameworks: Striking a fine balance between helicity and crystallinity. *Nano Res.* **2024**, *17*, 5726–5734.

[81] Li, X.; Loh, K. P. Recent progress in covalent organic frameworks as solid-state ion conductors. *ACS Mater. Lett.* **2019**, *1*, 327–335.

[82] Miner, E. M.; Dincă, M. Metal- and covalent-organic frameworks as solid-state electrolytes for metal-ion batteries. *Philos. Trans. A: Math. Phys. Eng. Sci.* **2019**, *377*, 20180225.

[83] Zhang, W. F.; Jiang, G. X.; Zou, W. W.; Zhang, L. H.; Li, S. L.; Qi, S. G.; Wang, X. J.; Cui, Z. M.; Song, H. Y.; Du, L. et al. Ionic covalent organic frameworks triggered efficient synergy: Li^+ de-solvation and the formation of LiF-rich interphase. *J. Power Sources* **2022**, *548*, 232001.

[84] Cheng, Q.; Jin, T. W.; Miao, Y. P.; Liu, Z.; Borovilas, J.; Zhang, H. R.; Liu, S. W.; Kim, S. Y.; Zhang, R. W.; Wang, H. Z. et al. Stabilizing lithium plating in polymer electrolytes by concentration-polarization-induced phase transformation. *Joule* **2022**, *6*, 2372–2389.

[85] Wei, S. H.; Wang, J. W.; Li, Y. Z.; Fang, Z. B.; Wang, L.; Xu, Y. X. Recent progress in COF-based electrode materials for rechargeable metal-ion batteries. *Nano Res.* **2023**, *16*, 6753–6770.

[86] Rong, L. Y.; Han, Y. F.; Zhang, C.; Yao, H. L.; He, Z. J.; Wang, X. B.; Guo, Z. P.; Mei, T. Regulating Li^+ transport and interfacial stability with zwitterionic COF protective layer towards high-performance lithium metal batteries. *Nano-Micro Lett.* **2026**, *18*, 163.

[87] Xu, J.; An, S. H.; Song, X. Y.; Cao, Y. J.; Wang, N.; Qiu, X.; Zhang, Y.; Chen, J. W.; Duan, X. L.; Huang, J. H. et al. Towards high performance Li-S batteries via sulfonate-rich COF-modified separator. *Adv. Mater.* **2021**, *33*, 2105178.

[88] Xu, J.; Tang, W. Q.; Yang, C.; Manke, I.; Chen, N.; Lai, F. L.; Xu, T.; An, S. H.; Liu, H. L.; Zhang, Z. L. et al. A highly conductive COF@CNT electrocatalyst boosting polysulfide conversion for Li–S chemistry. *ACS Energy Lett.* **2021**, *6*, 3053–3062.

[89] Hu, B.; Ding, B.; Xu, C.; Fan, Z. J.; Luo, D. R.; Li, P.; Dou, H.; Zhang, X. G. Fabrication of a covalent triazine framework functional interlayer for high-performance lithium-sulfur batteries. *Nanomaterials* **2022**, *12*, 255.

[90] Zhao, R. Y.; Wang, T.; Li, J. J.; Shi, Y. X.; Hou, M.; Yang, Y.; Zhang, Z. C.; Lei, S. B. Two-dimensional covalent organic frameworks for electrocatalysis: Achievements, challenges, and opportunities. *Nano Res.* **2023**, *16*, 8570–8595.

[91] Gao, Z. H.; Liu, Q.; Zhao, G. F.; Sun, Y. J.; Guo, H. Covalent organic frameworks for solid-state electrolytes of lithium metal batteries. *J. Mater. Chem. A* **2022**, *10*, 7497–7516.

[92] Meng, H. B.; Wu, B.; Sun, T. X.; Wei, L.; Zhang, Y. L.; Liu, B.; Chen, K.; Wang, Z. B.; Sun, S. H.; Wang, C. R. et al. Oxidization-induced structural optimization of Ni_3Fe-N-C derived from 3D covalent organic framework for high-efficiency and durable oxygen evolution reaction. *Nano Res.* **2023**, *16*, 6710–6720.

[93] Shan, Z.; Wu, M. M.; Du, Y. H.; Xu, B. Q.; He, B. Y.; Wu, X. W.; Zhang, G. Covalent organic framework-based electrolytes for fast Li^+ conduction and high-temperature solid-state lithium-ion batteries. *Chem. Mater.* **2021**, *33*, 5058–5066.

[94] Zheng, Z. J.; Ye, H.; Guo, Z. P. Recent progress on pristine metal/covalent-organic frameworks and their composites for lithium-sulfur batteries. *Energy Environ. Sci.* **2021**, *14*, 1835–1853.

[95] Feng, G. Y.; Li, X. J.; Zhang, M.; Xu, J. B.; Liu, Z. P.; Wu, L. L.;

Lei, S. B. Covalent organic framework monolayer: Accurate syntheses and advanced application. *Nano Res.* **2024**, *17*, 6603–6618.

[96] Cheng, M.; Zheng, S. B.; Sun, T. J.; Li, D. T.; Zhang, W. J.; Zha, Z. T.; Sun, Q.; Tian, J.; Zhang, K.; Tao, Z. L. A solubility limited pyrene-4,5,9,10-tetraone-based covalent organic framework for high-performance aqueous zinc-organic batteries. *Nano Res.* **2024**, *17*, 5095–5103.

[97] Deng, N. P.; Liu, Y. R.; Yu, W.; Kang, J. B.; Li, Q. X.; Gao, H. J.; Zhang, L. G.; Kang, W. M.; Liu, Y.; Cheng, B. W. Rational design and preparation of covalent organic frameworks and their functional mechanism analysis for lithium-ion and lithium sulfur/selenium cells. *Energy Storage Mater.* **2022**, *46*, 29–67.

[98] Zhang, T.; Zhang, G.; Chen, L. 2D conjugated covalent organic frameworks: Defined synthesis and tailor-made functions. *Acc. Chem. Res.* **2022**, *55*, 795–808.

[99] Yu, S. Y.; Zhao, G. F.; Zhu, H. Y.; Tang, H. L.; Hu, Q. X.; Luo, C. P.; Li, W. W.; An, Q.; Guo, H. Constructing donor–acceptor Li^+ transfer channels based on covalent organic frameworks for quasi-solid-state Li batteries. *Sci. China Chem.* **2025**, *68*, 6073–6082.

[100] Wang, W. K.; Zhao, W. W.; Xu, H. T.; Liu, S. J.; Huang, W.; Zhao, Q. Fabrication of ultra-thin 2D covalent organic framework nanosheets and their application in functional electronic devices. *Coord. Chem. Rev.* **2021**, *429*, 213616.

[101] Zhao, X. J.; Pachfule, P.; Thomas, A. Covalent organic frameworks (COFs) for electrochemical applications. *Chem. Soc. Rev.* **2021**, *50*, 6871–6913.

[102] Wang, X. X.; Chi, X. W.; Li, M. L.; Guan, D. H.; Miao, C. L.; Xu, J. J. An integrated solid-state lithium-oxygen battery with highly stable anionic covalent organic frameworks electrolyte. *Chem* **2023**, *9*, 394–410.

[103] Li, Z. E.; He, T.; Gong, Y. F.; Jiang, D. L. Covalent organic frameworks: Pore design and interface engineering. *Acc. Chem. Res.* **2020**, *53*, 1672–1685.

[104] Wu, H. M.; Ma, W. C.; Huang, X.; Cai, Y. F.; Li, J. H.; Liao, Q. B.; Xi, K.; Zhang, Q. H.; Jia, X. D. Single-ion quasi-solid-state electrolytes based on sulfonimide-functionalized covalent organic framework. *Polym. Chem.* **2024**, *15*, 4529–4541.

[105] Yusran, Y.; Fang, Q. R.; Valtchev, V. Electroactive covalent organic frameworks: Design, synthesis, and applications. *Adv. Mater.* **2020**, *32*, 2002038.

[106] Martínez-Abadía, M.; Mateo-Alonso, A. Structural approaches to control interlayer interactions in 2D covalent organic frameworks. *Adv. Mater.* **2020**, *32*, 2002366.

[107] Wang, H.; Wang, H.; Wang, Z. W.; Tang, L.; Zeng, G. M.; Xu, P.; Chen, M.; Xiong, T.; Zhou, C. Y.; Li, X. Y. et al. Covalent organic framework photocatalysts: Structures and applications. *Chem. Soc. Rev.* **2020**, *49*, 4135–4165.

[108] Lee, J. H.; Lee, H.; Lee, J.; Kang, T. W.; Park, J. H.; Shin, J. H.; Lee, H.; Majhi, D.; Lee, S. U.; Kim, J. H. Multicomponent covalent organic framework solid electrolyte allowing effective Li-ion dissociation and diffusion for all-solid-state batteries. *ACS Nano* **2023**, *17*, 17372–17382.

[109] Choi, R. H.; So, J.; Kim, Y.; Lee, D.; Byon, H. R. Li^+ conduction of soft-base anion-immobilized covalent organic frameworks for all-solid-state lithium-metal batteries. *ACS Energy Lett.* **2024**, *9*, 5341–5348.

[110] Kong, L. J.; Zhong, M.; Shuang, W.; Xu, Y. H.; Bu, X. H. Electrochemically active sites inside crystalline porous materials for energy storage and conversion. *Chem. Soc. Rev.* **2020**, *49*, 2378–2407.

[111] Huang, W.; Luo, W.; Li, Y. G. Two-dimensional semiconducting covalent organic frameworks for photocatalytic solar fuel production. *Mater. Today* **2020**, *40*, 160–172.

[112] Huang, X.; Sun, C.; Feng, X. Crystallinity and stability of covalent organic frameworks. *Sci. China Chem.* **2020**, *63*, 1367–1390.

[113] Zhao, G. F.; Ma, H.; Zhang, C. H.; Yang, Y. X.; Yu, S. Y.; Zhu, H. Y.; Sun, Y. J.; Guo, H. Constructing donor–acceptor-linked COFs electrolytes to regulate electron density and accelerate the Li^+ migration in quasi-solid-state battery. *Nano-Micro Lett.* **2025**, *17*, 21.

[114] Segura, J. L.; Mancheño, M. J.; Zamora, F. Covalent organic frameworks based on Schiff-base chemistry: Synthesis, properties and potential applications. *Chem. Soc. Rev.* **2016**, *45*, 5635–5671.

[115] Zhu, Q.; Wang, X.; Clowes, R.; Cui, P.; Chen, L. J.; Little, M. A.; Cooper, A. I. 3D cage COFs: A dynamic three-dimensional covalent organic framework with high-connectivity organic cage nodes. *J. Am. Chem. Soc.* **2020**, *142*, 16842–16848.

[116] Mi, S. J.; Geng, Y. Y.; Wang, Y. G.; Wang, C.; Yang, Z. W.; Zhao, F. L.; Li, Z. Functionalization of defective covalent organic frameworks for high-performance solid-state electrolytes. *Small* **2025**, *21*, e07272.

[117] Meng, J. C.; Yin, M. J.; Guo, K. R.; Zhou, X. P.; Xue, Z. G. *In situ* polymerization in COF boosts Li-ion conduction in solid polymer electrolytes for Li metal batteries. *Nano-Micro Lett.* **2025**, *17*, 248.

[118] Guo, D. H.; Shibuya, R.; Akiba, C.; Saji, S.; Kondo, T.; Nakamura, J. Active sites of nitrogen-doped carbon materials for oxygen reduction reaction clarified using model catalysts. *Science* **2016**, *351*, 361–365.

[119] Yang, Y. Z.; Schäfer, C.; Börjesson, K. Detachable all-carbon-linked 3D covalent organic framework films for semiconductor/COF heterojunctions by continuous flow synthesis. *Chem* **2022**, *8*, 2217–2227.

[120] Du, Y.; Yang, H. S.; Whiteley, J. M.; Wan, S.; Jin, Y. H.; Lee, S. H.; Zhang, W. Ionic covalent organic frameworks with spiroborate linkage. *Angew. Chem., Int. Ed.* **2016**, *55*, 1737–1741.

[121] Xu, J.; Yang, Y. T.; Dai, Q. Y.; Zheng, Z. Y.; Cao, Y. J.; Cheng, Y. W.; Peng, B.; Ma, L. B.; Wang, Y. G. Towards ultra-stable wide-temperature zinc-ion batteries by using ion-sieving organic framework membrane. *Angew. Chem., Int. Ed.* **2025**, *64*, e202423118.

[122] Meng, J. C.; Yin, M. J.; Li, F.; Guo, K. R.; Wang, Y.; Xue, Z. G. *In situ* orthogonal chemistry for facile preparation of uniform COF-based composite polymer electrolytes. *Angew. Chem., Int. Ed.* **2025**, *64*, e202515997.

[123] Zhang, Y. Y.; Duan, J. Y.; Ma, D.; Li, P. F.; Li, S. W.; Li, H. W.; Zhou, J. W.; Ma, X. J.; Feng, X.; Wang, B. Three-dimensional anionic cyclodextrin-based covalent organic frameworks. *Angew. Chem., Int. Ed.* **2017**, *56*, 16313–16317.

[124] Alcoutlabi, M.; McKenna, G. B. Effects of confinement on material behaviour at the nanometre size scale. *J. Phys.: Condens. Matter* **2005**, *17*, R461–R524.

[125] Zhang, C. H.; Zhao, L. W.; Li, F. K.; Song, X.; Chen, J. H.; Zeng, J.; Xi, L.; Hu, R. Z.; Zhu, M.; Liu, J. Optimizing the electron density of PVDF-HFP-based solid polymer electrolyte by donor-acceptor COF toward high-performance solid-state lithium metal batteries. *Adv. Mater.* **2025**, *37*, e13427.

[126] Wang, C.; Tang, J. D.; Chen, Z. Y.; Jin, Y. H.; Liu, J. B.; Xu, H.; Wang, H.; He, X. M.; Zhang, Q. Q. Ion-selective covalent organic frameworks boosting electrochemical energy storage and conversion: A review. *Energy Storage Mater.* **2023**, *55*, 498–516.

[127] Cui, M. Y.; Zhao, H. Y.; Qin, Y. Y.; Zhang, S. S.; Zhao, R. X.; Zhang, M.; Yu, W.; Gao, G. X.; Hu, X. F.; Su, Y. Q. et al. Regulation of lithium-ion flux by nanotopology lithiophilic boron-oxygen dipole in solid polymer electrolytes for lithium-metal batteries. *Energy Environ. Mater.* **2024**, *7*, e12659.

[128] Zhang, H. Y.; Geng, Y. B.; Huang, J.; Wang, Z. X.; Du, K.; Li, H. Y. Charge and mass transport mechanisms in two-dimensional covalent organic frameworks (2D COFs) for electrochemical energy storage devices. *Energy Environ. Sci.* **2023**, *16*, 889–951.

[129] Li, C.; Wang, D. D.; Poon Ho, G. S. H.; Zhang, Z. Y.; Huang, J.; Bang, K. T.; Lau, C. Y.; Leu, S. Y.; Wang, Y. M.; Kim, Y. Anthraquinone-based silicate covalent organic frameworks as solid electrolyte interphase for high-performance lithium-metal batteries. *J. Am. Chem. Soc.* **2023**, *145*, 24603–24614.

[130] Park, S. S.; Tulchinsky, Y.; Dincă, M. Single-ion Li^+, Na^+, and Mg^{2+} solid electrolytes supported by a mesoporous anionic Cu-azolate metal-organic framework. *J. Am. Chem. Soc.* **2017**, *139*, 13260–13263.

[131] Duan, S.; Qian, L. T.; Zheng, Y.; Zhu, Y. F.; Liu, X.; Dong, L.; Yan, W.; Zhang, J. J. Mechanisms of the accelerated Li^+ conduction in MOF-based solid-state polymer electrolytes for all-solid-state lithium metal batteries. *Adv. Mater.* **2024**, *36*, 2314120.

[132] Jiang, S. S.; Wang, J. Z.; Yang, G. X.; Chen, J. L.; Li, R. H.; Fan, X. L.; Li, Z. T. Tailoring lithium-ion coordination in metal-organic frameworks via d-orbital control for fast ion conduction. *J. Am. Chem. Soc.* **2026**, *148*, 2481–2490.

[133] Lu, G. L.; Meng, G.; Liu, Q.; Feng, L. G.; Luo, J.; Liu, X. J.; Luo, Y.; Chu, P. K. Advanced strategies for solid electrolyte interface design with MOF materials. *Adv. Powder Mater.* **2024**, *3*, 100154.

[134] Lee, J.; Shin, J. H.; Hong, S.; Lee, J. H.; Jeong, D. H.; Kim, H.; Kim, Y. H.; Lee, S. U.; Kim, J. H. Eutectic-like ion-conductive phase-incorporated zwitterionic covalent organic framework solid electrolyte for all-solid-state Li metal batteries. *Adv. Sci.* **2025**, *12*, e05530.

[135] Zhang, K. C.; Zhang, B. K.; Weng, M. Y.; Zheng, J. X.; Li, S. N.; Pan, F. Lithium ion diffusion mechanism in covalent organic framework based solid state electrolyte. *Phys. Chem. Chem. Phys.* **2019**, *21*, 9883–9888.

[136] Liu, T. T.; Zhong, Y.; Yan, Z. W.; He, B. Y.; Liu, T.; Ling, Z. Y.; Li, B. C.; Liu, X.; Zhu, J. L.; Jiang, L. Y. et al. Fabrication of scalable covalent organic framework membrane-based electrolytes for solid-state lithium metal batteries. *Angew. Chem., Int. Ed.* **2024**, *63*, e202411535.

[137] Chen, H. W.; Tu, H. Y.; Hu, C. J.; Liu, Y.; Dong, D. R.; Sun, Y. F.; Dai, Y. F.; Wang, S. L.; Qian, H.; Lin, Z. Y. et al. Cationic covalent organic framework nanosheets for fast Li-ion conduction. *J. Am. Chem. Soc.* **2018**, *140*, 896–899.

[138] Li, X.; Hou, Q.; Huang, W.; Xu, H. S.; Wang, X. W.; Yu, W.; Li, R. L.; Zhang, K.; Wang, L.; Chen, Z. X. et al. Solution-processable covalent organic framework electrolytes for all-solid-state Li-organic batteries. *ACS Energy Lett.* **2020**, *5*, 3498–3506.

[139] Niu, C. Q.; Luo, W. J.; Dai, C. M.; Yu, C. B.; Xu, Y. X. High-voltage-tolerant covalent organic framework electrolyte with holistically oriented channels for solid-state lithium metal batteries with nickel-rich cathodes. *Angew. Chem., Int. Ed.* **2021**, *60*, 24915–24923.

[140] Liu, J.; Zhang, Y. H.; Ji, H. Q.; Zhang, J.; Zhou, P. X.; Cao, Y. F.; Zhou, J. Q.; Yan, C. L.; Qian, T. Cationic covalent organic framework with ultralow HOMO energy used as scaffolds for 5.2 V solid polycarbonate electrolytes. *Adv. Sci.* **2022**, *9*, 2200390.

[141] Kang, T. W.; Lee, J. H.; Lee, J.; Park, J. H.; Shin, J. H.; Ju, J. M.; Lee, H.; Lee, S. U.; Kim, J. H. An ion-channel-restructured zwitterionic covalent organic framework solid electrolyte for all-solid-state lithium-metal batteries. *Adv. Mater.* **2023**, *35*, 2301308.

[142] Yuan, Y. F.; Zhang, Z. Y.; Zhang, Z. Y.; Bang, K. T.; Tian, Y.; Dang, Z. Z.; Gu, M. H.; Wang, R.; Tao, R.; Lu, Y. Y. et al. Highly conductive imidazolate covalent organic frameworks with ether chains as solid electrolytes for lithium metal batteries. *Angew. Chem., Int. Ed.* **2024**, *63*, e202402202.

[143] Guan, D. H.; Wang, X. X.; Li, L.; Chen, G. N.; Qiao, G. Y.; Xu, J. J. Homologous imide bonds to build polymer-covalent organic framework electrolytes for efficient ion transport. *J. Am. Chem. Soc.* **2025**, *147*, 38078–38088.

[144] Vazquez-Molina, D. A.; Mohammad-Pour, G. S.; Lee, C.; Logan, M. W.; Duan, X. F.; Harper, J. K.; Uribe-Romo, F. J. Mechanically shaped two-dimensional covalent organic frameworks reveal crystallographic alignment and fast Li-ion conductivity. *J. Am. Chem. Soc.* **2016**, *138*, 9767–9770.

[145] Ashraf, S.; Zuo, Y. M.; Li, S.; Liu, C. X.; Wang, H.; Feng, X.; Li, P. F.; Wang, B. Crystalline anionic germanate covalent organic framework for high CO_2 selectivity and fast Li ion conduction. *Chem.—Eur. J.* **2019**, *25*, 13479–13483.

[146] Zhang, G.; Hong, Y. L.; Nishiyama, Y.; Bai, S. Y.; Kitagawa, S.; Horike, S. Accumulation of glassy poly(ethylene oxide) anchored in a covalent organic framework as a solid-state Li^+ electrolyte. *J. Am. Chem. Soc.* **2019**, *141*, 1227–1234.

[147] Xu, Q.; Tao, S. S.; Jiang, Q. H.; Jiang, D. L. Ion conduction in polyelectrolyte covalent organic frameworks. *J. Am. Chem. Soc.* **2018**, *140*, 7429–7432.

[148] Jeong, K.; Park, S.; Jung, G. Y.; Kim, S. H.; Lee, Y. H.; Kwak, S. K.; Lee, S. Y. Solvent-free, single lithium-ion conducting covalent organic frameworks. *J. Am. Chem. Soc.* **2019**, *141*, 5880–5885.

[149] Li, Z.; Liu, Z. W.; Mu, Z. J.; Cao, C.; Li, Z. Y.; Wang, T. X.; Li, Y.; Ding, X. S.; Han, B. H.; Feng, W. Cationic covalent organic framework based all-solid-state electrolytes. *Mater. Chem. Front.* **2020**, *4*, 1164–1173.

[150] Li, Z.; Liu, Z.W.; Li, Z. Y.; Wang, T. X.; Zhao, F. L.; Ding, X. S.; Feng, W.; Han, B. H. Defective 2D covalent organic frameworks for postfunctionalization. *Adv. Funct. Mater.* **2020**, *30*, 1909267.

[151] Hu, Y. M.; Dunlap, N.; Wan, S.; Lu, S. L.; Huang, S. F.; Sellinger, I.; Ortiz, M.; Jin, Y. H.; Lee, S. H.; Zhang, W. Crystalline lithium imidazolate covalent organic frameworks with high Li-ion conductivity. *J. Am. Chem. Soc.* **2019**, *141*, 7518–7525.

[152] Liu, Z. Y.; Zhang, K.; Huang, G. J.; Bian, S. Y.; Huang, Y.; Jiang, X. Z.; Pan, Y. Y.; Wang, Y. X.; Xia, X. F.; Xu, B. Q. et al. Lithium-ion transport in covalent organic framework membrane. *Chem. Eng. J.* **2022**, *433*, 133550.

[153] Park, M.; Zhang, X. C.; Chung, M.; Less, G. B.; Sastry, A. M. A review of conduction phenomena in Li-ion batteries. *J. Power Sources* **2010**, *195*, 7904–7929.

[154] Cao, Y.; Wang, M. D.; Wang, H. J.; Han, C. Y.; Pan, F. S.; Sun, J. Covalent organic framework for rechargeable batteries: Mechanisms and properties of ionic conduction. *Adv. Energy Mater.* **2022**, *12*, 2200057.

[155] Ding, H. M.; Mal, A.; Wang, C. Energy storage in covalent organic frameworks: From design principles to device integration. *Chem. Res. Chin. Univ.* **2022**, *38*, 356–363.

[156] Dey, A.; Ramlal, V. R.; Sankar, S. S.; Kundu, S.; Mandal, A. K.; Das, A. Self-assembled cationic organic nanosheets: Role of positional isomers in a guanidinium-core for efficient lithium-ion conduction. *Chem. Sci.* **2021**, *12*, 13878–13887.

[157] Cheng, Z. Z.; Lu, L. P.; Zhang, S. Y.; Liu, H. Y.; Xing, T.; Lin, Y.; Ren, H.; Li, Z. T.; Zhi, L. J.; Wu, M. B. Amphoteric covalent organic framework as single Li^+ superionic conductor in all-solid-state. *Nano Res.* **2023**, *16*, 528–535.

[158] Dong, D. R.; Zhang, H.; Zhou, B.; Sun, Y. F.; Zhang, H. L.; Cao, M.; Li, J. B.; Zhou, H.; Qian, H.; Lin, Z. Y. et al. Porous covalent organic frameworks for high transference number polymer-based electrolytes. *Chem. Commun.* **2019**, *55*, 1458–1461.

[159] Li, P. Y.; Lv, H. W.; Li, Z. L.; Meng, X. P.; Lin, Z.; Wang, R. H.; Li, X. J. The electrostatic attraction and catalytic effect enabled by ionic-covalent organic nanosheets on MXene for separator modification of lithium-sulfur batteries. *Adv. Mater.* **2021**, *33*, 2007803.

[160] Cao, Y.; Wu, H.; Li, G.; Liu, C.; Cao, L.; Zhang, Y. M.; Bao, W.; Wang, H. L.; Yao, Y.; Liu, S. et al. Ion selective covalent organic framework enabling enhanced electrochemical performance of lithium-sulfur batteries. *Nano Lett.* **2021**, *21*, 2997–3006.

[161] Zhao, G. F.; Mei, Z. Y.; Duan, L. Y.; An, Q.; Yang, Y. X.; Zhang, C. H.; Tan, X. P.; Guo, H. COF-based single Li^+ solid electrolyte accelerates the ion diffusion and restrains dendrite growth in quasi-solid-state organic batteries. *Carbon Energy* **2023**, *5*, e248.

[162] Sun, Y. J.; Zhao, G. F.; Fu, Y.; Yang, Y. X.; Zhang, C. H.; An, Q.; Guo, H. Understanding a single-Li-ion COF conductor for being dendrite free in a Li-organic battery. *Research* **2022**, *2022*, 9798582.

[163] Wang, Y.; Geng, S. Q.; Yan, G. J.; Liu, X. N.; Zhang, X. J.; Feng, Y.; Shi, J. J.; Qu, X. W. A squaraine-linked zwitterionic covalent

organic framework nanosheets enhanced poly(ethylene oxide) composite polymer electrolyte for quasi-solid-state Li-S batteries. *ACS Appl. Energy Mater.* **2022**, *5*, 2495–2504.

[164] Guo, D.; Shinde, D. B.; Shin, W.; Abou-Hamad, E.; Emwas, A. H.; Lai, Z. P.; Manthiram, A. Foldable solid-state batteries enabled by electrolyte mediation in covalent organic frameworks. *Adv. Mater.* **2022**, *34*, 2201410.

[165] Tian, X. L.; Chen, S. H.; Zhang, P.; Yang, P.; Yi, Y. K.; Wang, T.; Fang, B. R.; Liu, P.; Qu, L.; Li, M. T. et al. Covalent organic frameworks with immobilized anions to liberate lithium ions: Quasi-solid electrolytes with enhanced rate capabilities. *Electrochim. Acta* **2021**, *389*, 138585.

[166] Sun, W. L.; Zhang, J. S.; Xie, M. L.; Lu, D. R.; Zhao, Z.; Li, Y. Q.; Cheng, Z. Y.; Zhang, S. J.; Chen, H. W. Ultrathin aramid/COF heterolayered membrane for solid-state Li-metal batteries. *Nano Lett.* **2020**, *20*, 8120–8126.

[167] Zhang, K. G.; Niu, C. Q.; Yu, C. B.; Zhang, L.; Xu, Y. X. Highly crystalline vinylene-linked covalent organic frameworks enhanced solid polycarbonate electrolyte for dendrite-free solid lithium metal batteries. *Nano Res.* **2022**, *15*, 8083–8090.

[168] Wang, Y. X.; Zhang, K.; Jiang, X. Z.; Liu, Z. Y.; Bian, S. Y.; Pan, Y. Y.; Shan, Z.; Wu, M. M.; Xu, B. Q.; Zhang, G. Branched poly(ethylene glycol)-functionalized covalent organic frameworks as solid electrolytes. *ACS Appl. Energy Mater.* **2021**, *4*, 11720–11725.

[169] Lin, Z. H.; Wang, Y.; Li, Y.; Liu, Y.; Zhong, S. C.; Xie, M. S.; Yan, F.; Zhang, Z. Y.; Peng, J.; Li, J. Q. et al. Regulating solvation structure in gel polymer electrolytes with covalent organic frameworks for lithium metal batteries. *Energy Storage Mater.* **2022**, *53*, 917–926.

[170] Zhao, G. F.; Xu, L. F.; Jiang, J. W.; Mei, Z. Y.; An, Q.; Lv, P. P.; Yang, X. F.; Guo, H.; Sun, X. L. COFs-based electrolyte accelerates the Na^+ diffusion and restrains dendrite growth in quasi-solid-state organic batteries. *Nano Energy* **2022**, *92*, 106756.

[171] Yu, J. T.; Hu, Y.; Ma, X. Y.; Zou, X. Y.; Qi, H. J.; Zhou, Y. J.; Yan, F. A highly conductive and stable hybrid solid electrolyte for high voltage lithium metal batteries. *J. Mater. Chem. A* **2022**, *10*, 12842–12855.

[172] Liu, Z. Y.; Zhang, K.; Huang, G. J.; Xu, B. Q.; Hong, Y. L.; Wu, X. W.; Nishiyama, Y.; Horike, S.; Zhang, G.; Kitagawa, S. Highly processable covalent organic framework gel electrolyte enabled by side-chain engineering for lithium-ion batteries. *Angew. Chem., Int. Ed.* **2022**, *61*, e202110695.

[173] Cheng, Z. Y.; Xie, M. L.; Mao, Y. Y.; Ou, J. X.; Zhang, S. J.; Zhao, Z.; Li, J. L.; Fu, F.; Wu, J. H. et al. Building lithiophilic ion-conduction highways on garnet-type solid-state Li^+ conductors. *Adv. Energy Mater.* **2020**, *10*, 1904230.

[174] Zhang, Y. C.; Wu, Y.; Liu, Y. P.; Feng, J. K. Flexible and freestanding heterostructures based on COF-derived N-doped porous carbon and two-dimensional MXene for all-solid-state lithium-sulfur batteries. *Chem. Eng. J.* **2022**, *428*, 131040.

[175] Guo, Z. B.; Zhang, Y. Y.; Dong, Y.; Li, J.; Li, S. W.; Shao, P. P.; Feng, X.; Wang, B. Fast ion transport pathway provided by polyethylene glycol confined in covalent organic frameworks. *J. Am. Chem. Soc.* **2019**, *141*, 1923–1927.

[176] Wu, M. M.; Huang, H. R.; Xu, B. Q.; Zhang, G. Poly(ethylene glycol)-functionalized 3D covalent organic frameworks as solid-state polyelectrolytes. *RSC Adv.* **2022**, *12*, 16354–16357.

[177] Wang, S.; Li, X. C.; Cheng, T.; Liu, Y. Y.; Li, Q. G.; Bai, M. L.; Liu, X.; Geng, H. G.; Lai, W. Y.; Huang, W. Highly conjugated three-dimensional covalent organic frameworks with enhanced Li-ion conductivity as solid-state electrolytes for high-performance lithium metal batteries. *J. Mater. Chem. A* **2022**, *10*, 8761–8771.

[178] Zheng, S.; Bi, S.; Fu, Y. B.; Wu, Y.; Liu, M. H.; Xu, Q.; Zeng, G. F. 3D crown ether covalent organic framework as interphase layer toward high-performance lithium metal batteries. *Adv. Mater.* **2024**, *36*, 2313076.

[179] Yin, Y.; Zhang, Y.; Zhou, X.; Gui, B.; Wang, W. Q.; Jiang, W. T.; Zhang, Y. B.; Sun, J. L.; Wang, C. Ultrahigh-surface area covalent organic frameworks for methane adsorption. *Science* **2024**, *386*, 693–696.

[180] Ding, H. M.; Zhang, Y.; Wang, Z. X.; Du, H. L.; Li, M. S.; Huang, X. Y.; Zhou, X.; Zhang, Z. Y.; Wu, Z. H.; Li, W. X. et al. Absolute configuration control in covalent organic frameworks. *J. Am. Chem. Soc.* **2025**, *147*, 29359–29366.